A RADIAL AND TANGENTIAL FRAMEWORK FOR STUDYING TRANSIENT REACTIVITY

JAMES $BRODA^1$, ALANNA $HASLAM-HYDE^{2,*}$, AND MARY LOU ZEEMAN³

¹Washington and Lee University, Department of Mathematics ²Boston University, Department of Mathematics and Statistics ³Bowdoin College, Department of Mathematics *Corresponding Author; ajhaslam@bu.edu

1. Introduction. It is a surprising, albeit well-known, fact that even a linear system of ordinary differential equations (ODE), with a global attractor at the origin, may have trajectories that move away from the origin before eventually converging there. See Figure 1. No nonlinearity or degeneracy is needed in the system for this transient amplification of perturbations from the equilibrium to occur. For example, the ODE system presented below exhibits this behavior, which is illustrated in Figure 1.

$$\frac{dx}{dt} = -x - 8y$$

$$\frac{dy}{dt} = -3y \tag{1.1}$$

In their landmark paper [1], Neubert and Caswell coined the term *reactivity* to capture the maximal rate of radial amplification of perturbations as follows:

Definition 1.1. Given a real $n \times n$ matrix A, consider the linear system

$$\frac{dX}{dt} = AX\tag{1.2}$$

For any initial condition $X_0 \in \mathbb{R}^n$, let X(t) be the solution of the system with $X(0) = X_0$, let r(t) = ||X(t)||, and let $r_0 = ||X_0||$.

The reactivity, ρ , of System (1.2) is given by

$$\rho = \max_{X_0 \neq 0} \left(\frac{1}{r_0} \frac{dr}{dt} \Big|_{t=0} \right) \tag{1.3}$$

and the system is called reactive if $\rho > 0$.

Neubert and Caswell [1] show that reactivity is equal to the largest eigenvalue of the symmetric part of A. Equivalently,

$$\rho = \max(\lambda(H_A))$$

where $H_A = \frac{1}{2}(A + A^T)$ is the symmetric, or Hermitian, part of A, and $\lambda(H_A)$ denotes the set of eigenvalues of H_A . To characterize the extent to which reactivity is seen in the transient amplification of solutions, Neubert and Caswell introduce the concept of maximal amplification, ρ_{max} , which measures the largest possible growth factor attained by a perturbation to the origin. Also of interest is the time needed to achieve maximal amplification, t_{max} , which is illustrated in Figure 1.

In analogy with reactivity, Townley and Hodgson [2] introduce *attenuation* as the minimum rate of radial amplification of perturbations. System (1.2) is then called

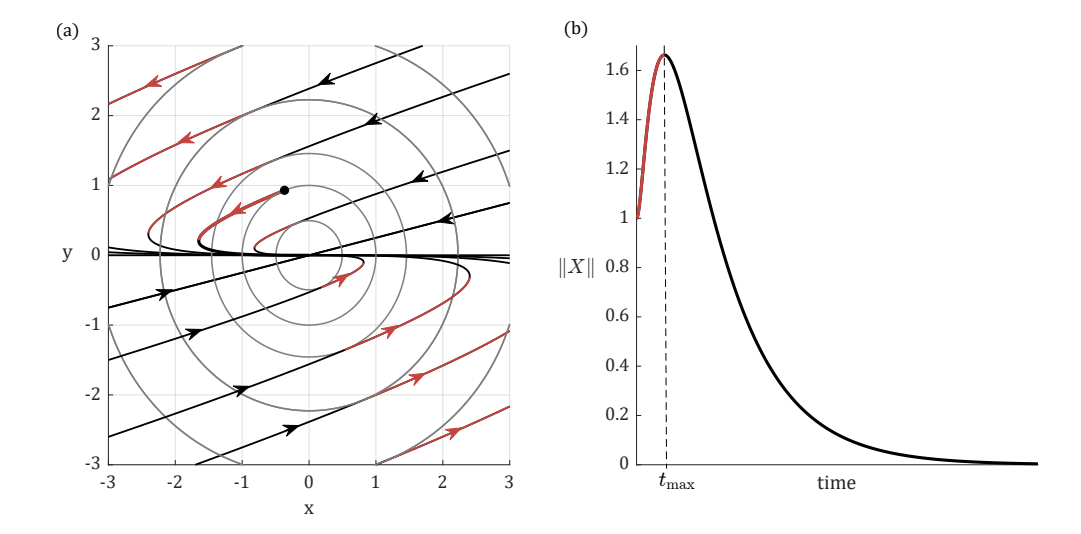


Fig. 1: (a) The phase portrait of linear ODE with coefficient matrix $A = \begin{pmatrix} -1 & -8 \\ 0 & -3 \end{pmatrix}$ is plotted with concentric circles in grey indicating contours of equal distance from the origin. Many trajectories exhibit reactive transient growth (highlighted in red) away from the origin before being asymptotically attracted. The solution trajectory with initial condition $(x,y)\approx (-0.4,0.9)$ on the unit circle is selected to illustrate maximum amplification. (b) The distance of this selected trajectory from the origin is plotted versus time with transient amplification highlighted in red. The trajectory is amplified from t=0 to $t=t_{\rm max}$ where it attains maximum amplification $\rho_{\rm max}\approx 1.67$.

attenuating if the attenuation is negative, corresponding to (possibly transient) radial decay of solutions.

In this paper we introduce a novel way to calculate the reactivity and attenuation of System (1.2) when A is 2×2 , by decomposing the vector field AX into its radial and tangential components. The decomposition sheds new light on the interplay between the eigen- and reactivity structures of the system, thereby revealing interesting parallels between its transient and asymptotic behaviors.

The surprising consequences of reactivity are known in many fields of mathematics. Neubert and Caswell [1] were motivated by the study of resilience of ecological systems to perturbations - a subject that becomes ever more important as climate change and human activities deliver new disturbance patterns to those systems.

Harrington et al. consider reactivity and attenuation (in the l_1 and l_2 norms), in the context of marine metapopulations. Within their family of models, they show that even for 2×2 matrices, the asymptotic and transient dynamics of System (1.2) can be strikingly different, with the populations growing arbitrarily large (through reactivity) before eventually going extinct, or decaying to arbitrarily small levels (through attenuation) before eventually growing. Long transients such as these can present significant challenges for sustainable ecosystem management [3, 4]. To study the resilience of ecological (and other) systems to repeated perturbation, Meyer et al. [5] define flow-kick systems, in which the solution (flow) of an ordinary differential equation is regularly subjected to instantaneous state perturbations (kicks). They show that if the resulting flow-kick system equilibrates, then the stability properties of the flow-kick equilibrium are governed by the variational equation; a nonautonomous linear differential equation capturing the net impact (over time) of the perturbations; see also [6].

In the context of nonautonomous systems, recent scholarship [7, 8, 9] has highlighted how solutions to X'(t) = B(t)X can grow without bound even when the time-varying coefficient matrix B(t) always has eigenvalues with negative real part. The critical idea is that transient reactivity can accumulate in nonautonomous systems. We note that most undergraduate courses in Control Theory cover transient analysis; however, the typical approaches rely on either Laplace Transforms or numerical simulation, and the underlying dynamics are typically higher order; see [10] and [11]. In undergraduate ODE courses, transient analysis is often emphasized less than steady-state eigenvalue analysis. When introducing linear ODEs, steady-state analysis centers on the diagonalized form of the coefficient matrix, which loses important information about the transient behavior. If A is diagonal with negative eigenvalues, then System (1.2) cannot be reactive. Thus, as Higham and Trefethan [12] point out, important information about the dynamics of ODEs is lost not only through the process of linearization or freezing nonautonomous coefficients, but also through the process of diagonalization. Guided by geometric intuition, we develop a framework and an accompanying matrix decomposition to facilitate analysis of transient behavior in linear systems, even in the nonautonomous case.

Overview of the Paper. In Section 2, we present Theorem 2.1, in which we use polar coordinates to decompose a two-dimensional linear vector field into its radial and tangential components, \mathcal{R} and \mathcal{T} , respectively. This simple decomposition is the cornerstone of the paper. In the corollaries that follow, we describe the structure of the decomposition, and its surprisingly many consequences for illuminating the dynamics and reactivity of a two-dimensional linear system (System (2.1)). Given the novelty of our approach, we provide detailed proofs for both Theorem 2.1 and subsequent corollaries.

In Section 3, we expand on the ideas of reactivity and attenuation, using the radial component, \mathcal{R} , to define reactive and attenuating regions of the system. In Section 4 we view the eigen-structure of the system through the lens of \mathcal{R} and \mathcal{T} . This paves the way for a matching structure of orthovectors and orthovalues, defined in Section 5, that describes properties of the reactive region.

In Section 6, inspired by the observation of Higham and Trefethan [12] that diagonalization masks any transient reactivity or attenuation of systems, we propose four standard matrix forms that are easy to calculate and that illuminate transient dynamics. Each of these standard forms results from conjugation by pure rotation, and hence respects both the transient and asymptotic behavior of a system.

In Section 7, we use our standard forms to explore the limits of reactivity and maximal amplification in linear systems. In reactive systems with an attracting origin, we demonstrate that for a given pair of eigenvectors, maximal amplification is bounded, but reactivity can be arbitrarily large.

In Section 8, we use our reactivity framework to develop examples of nonautonomous linear systems in which the origin is attracting at all moments in time, and yet solutions can drift arbitrarily far away.

2. Accessing radial dynamics directly. We are interested in reactivity and the transient movement of trajectories away from the origin. To access the radial dynamics directly, we write the Cartesian coordinates of $X \in \mathbb{R}^2$ in terms of the polar coordinates (r, θ) , where $r = ||X|| \ge 0$ and $\theta \in \mathbb{R} \pmod{2\pi}$ measures the counter-clockwise angle of X from the x-axis. Thus, we consider the two-dimensional

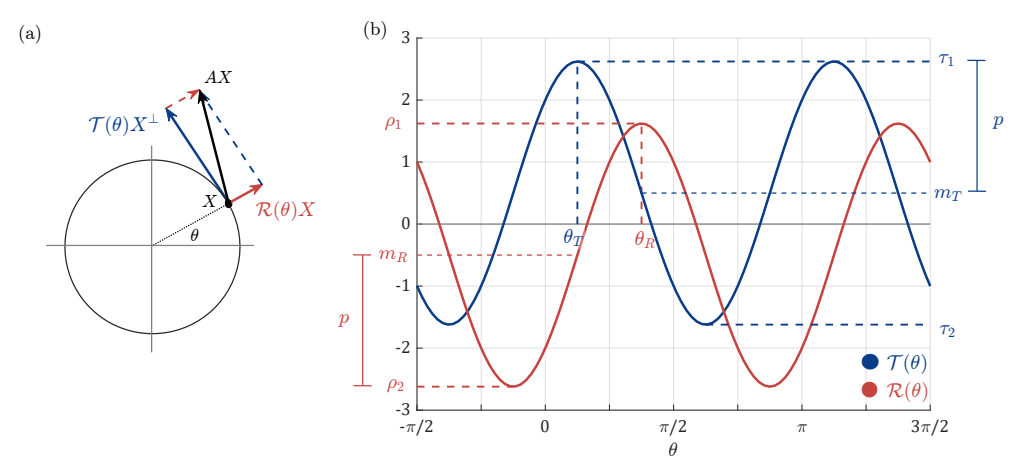


Fig. 2: (a) The vector field defined by AX is decomposed in to components in the direction radial to and tangential to the vector X. The radial component, in red, and the tangential component, in dark blue, are both given as functions of the angle θ . (b) Graphs of \mathcal{R} and \mathcal{T} as functions of θ . Each is sinusoidal with period π and amplitude p. \mathcal{R} , in red, has maximum and minimum values ρ_1 and ρ_2 , respectively, midline m_R and maximum at θ_R . \mathcal{T} , in dark blue, has maximum and minimum values τ_1 and τ_2 , respectively, midline m_T and maximum at $\theta_T = \theta_R - \pi/4$. See Corollary 2.4.

autonomous linear system of ordinary differential equations:

$$\frac{dX}{dt} = AX, \text{ where } X = \begin{pmatrix} x_1 \\ x_2 \end{pmatrix} = \begin{pmatrix} r\cos\theta \\ r\sin\theta \end{pmatrix} \in \mathbb{R}^2 \text{ and } A = \begin{pmatrix} a_{11} & a_{12} \\ a_{21} & a_{22} \end{pmatrix}$$
 (2.1)

Radial and tangential components of AX. Theorem 2.1, below, teases apart the radial and tangential components of the vector field AX, each of which depends solely on θ (a consequence of linearity). See Figure 2. This straightforward decomposition of AX is surprisingly illuminating and provides the foundation on which we build insight into the structure of reactivity in two-dimensional linear systems. First, we introduce some notation that will be used throughout the paper.

NOTATION. Let J and J^{-1} be the matrices representing counter-clockwise and clockwise rotation by $\pi/2$ radians in \mathbb{R}^2 , respectively. For $X = \begin{pmatrix} x_1 \\ x_2 \end{pmatrix} \in \mathbb{R}^2$, let X^{\perp} denote the vector orthogonal to X obtained by counter-clockwise rotation by $\pi/2$:

$$J = \begin{pmatrix} 0 & -1 \\ 1 & 0 \end{pmatrix}, \quad J^{-1} = -J = \begin{pmatrix} 0 & 1 \\ -1 & 0 \end{pmatrix}, \text{ and } X^{\perp} = JX = \begin{pmatrix} -x_2 \\ x_1 \end{pmatrix} \tag{2.2}$$

Theorem 2.1. Given real
$$A=\begin{pmatrix} a_{11} & a_{12} \\ a_{21} & a_{22} \end{pmatrix}$$
 and $X=\begin{pmatrix} r\cos\theta \\ r\sin\theta \end{pmatrix},\ r\geq0,\ \theta\in$

 $\mathbb{R} \pmod{2\pi}$, the vector $AX \in \mathbb{R}^2$ can be decomposed into components parallel and orthogonal to X by:

$$AX = \mathcal{R}(\theta)X + \mathcal{T}(\theta)X^{\perp}, \tag{2.3}$$

where $\mathcal{R}(\theta)$ and $\mathcal{T}(\theta)$ are real-valued functions given by

$$\mathcal{R}(\theta) = m_R + p\cos(2(\theta - \theta_R)) \tag{2.4}$$

$$\mathcal{T}(\theta) = m_T - p\sin(2(\theta - \theta_R)) \tag{2.5}$$

with

$$m_R = \frac{1}{2}(a_{11} + a_{22}) \tag{2.6}$$

$$m_T = \frac{1}{2}(a_{21} - a_{12}) \tag{2.7}$$

$$p = \frac{1}{2}\sqrt{(a_{11} - a_{22})^2 + (a_{12} + a_{21})^2}$$
 (2.8)

and, if $p \neq 0$,

$$\theta_R = \frac{1}{2}\arctan(a_{12} + a_{21}, a_{11} - a_{22}) \in \mathbb{R} \pmod{\pi}$$
 (2.9)

REMARK. We use the two-argument form of $\arctan(y,x) \in \mathbb{R} \pmod{2\pi}$ to ensure that θ_R is well-defined in $\mathbb{R} \pmod{\pi}$. This is the appropriate space for θ_R to be defined in due to the π -periodicity of \mathcal{R} and \mathcal{T} which will be addressed in Corollary 2.4.

The r-independence of the radial and tangential decomposition in Theorem 2.1 is a consequence of the linearity of the system. Along radial lines in \mathbb{R}^2 , the vector field is just scaled by the radius. Therefore we can restrict attention to the unit circle S^1 (i.e. $r = 1, \theta \in \mathbb{R} \pmod{2\pi}$) and study properties of the vector field (and its associated dynamics) on all of \mathbb{R}^2 through the single variable functions $\mathcal{R}(\theta)$ and $\mathcal{T}(\theta)$. First, we prove Theorem 2.1 and show, in Corollary 2.2, that we can recover the matrix A from the functions \mathcal{R} and \mathcal{T} .

Proof of Theorem 2.1. Projecting AX onto the X and X^{\perp} directions, we have

$$\begin{split} AX &= \left(AX \cdot \frac{X}{\|X\|}\right) \frac{X}{\|X\|} + \left(AX \cdot \frac{X^{\perp}}{\|X^{\perp}\|}\right) \frac{X^{\perp}}{\|X^{\perp}\|} \\ &= \left(\frac{AX \cdot X}{\|X\|^2}\right) X + \left(\frac{AX \cdot X^{\perp}}{\|X^{\perp}\|^2}\right) X^{\perp}. \end{split}$$

Thus, the coefficient of X in Equation (2.3) is given by:

$$\begin{pmatrix} \frac{AX \cdot X}{\|X\|^2} \end{pmatrix} = \frac{1}{r^2} \begin{pmatrix} a_{11} & a_{12} \\ a_{21} & a_{22} \end{pmatrix} \begin{pmatrix} r \cos \theta \\ r \sin \theta \end{pmatrix} \cdot \begin{pmatrix} r \cos \theta \\ r \sin \theta \end{pmatrix}$$

$$= a_{11} \cos^2 \theta + (a_{12} + a_{21}) \cos \theta \sin \theta + a_{22} \sin^2 \theta.$$

Invoking double-angle identities, we have:

$$\left(\frac{AX \cdot X}{\|X\|^2}\right) = \frac{1}{2} \left(a_{11} (\cos(2\theta) + 1) + (a_{12} + a_{21}) \sin(2\theta) + a_{22} (1 - \cos(2\theta)) \right)$$
$$= \frac{1}{2} \left((a_{11} + a_{22}) + (a_{11} - a_{22}) \cos(2\theta) + (a_{12} + a_{21}) \sin(2\theta) \right)$$

Using the Pythagorean Theorem, we can express this coefficient as a single sinusoid,

$$\left(\frac{AX \cdot X}{\|X\|^2}\right) = m_R + p\cos(2(\theta - \theta_R)) = \mathcal{R}(\theta),$$

where p and θ_R are given by Equations 2.8 and 2.9. Similarly, $||X^{\perp}|| = ||X|| = r$, and

the coefficient of X^{\perp} in Equation (2.3) is given by:

$$\left(\frac{AX \cdot X^{\perp}}{\|X^{\perp}\|^{2}}\right) = \frac{1}{r^{2}} \begin{pmatrix} a_{11} & a_{12} \\ a_{21} & a_{22} \end{pmatrix} \begin{pmatrix} r \cos \theta \\ r \sin \theta \end{pmatrix} \cdot \begin{pmatrix} -r \sin \theta \\ r \cos \theta \end{pmatrix}
= (a_{22} - a_{11}) \cos \theta \sin \theta - a_{12} \sin^{2} \theta + a_{21} \cos^{2} \theta
= \frac{1}{2} ((a_{21} - a_{12}) + (a_{12} + a_{21}) \cos(2\theta) + (a_{22} - a_{11}) \sin(2\theta))
= m_{T} - p \sin(2(\theta - \theta_{R}))
= \mathcal{T}(\theta).$$

Thus $AX = \mathcal{R}(\theta)X + \mathcal{T}(\theta)X^{\perp}$.

COROLLARY 2.2. Given real $A = \begin{pmatrix} a_{11} & a_{12} \\ a_{21} & a_{22} \end{pmatrix}$ and $\mathcal{R}(\theta), \mathcal{T}(\theta)$ as in Theorem 2.1,

$$A = \begin{pmatrix} \mathcal{R}(0) & -\mathcal{T}(\pi/2) \\ \mathcal{T}(0) & \mathcal{R}(\pi/2) \end{pmatrix}$$

Proof. Consider $X = \begin{pmatrix} \cos \theta \\ \sin \theta \end{pmatrix} \in S^1$. At $\theta = 0$, $X = \begin{pmatrix} 1 \\ 0 \end{pmatrix}$ and $X^{\perp} = \begin{pmatrix} 0 \\ 1 \end{pmatrix}$. Thus, by Theorem 2.1,

$$A\begin{pmatrix} 1\\0 \end{pmatrix} = \mathcal{R}(0)\begin{pmatrix} 1\\0 \end{pmatrix} + \mathcal{T}(0)\begin{pmatrix} 0\\1 \end{pmatrix} = \begin{pmatrix} \mathcal{R}(0)\\\mathcal{T}(0) \end{pmatrix}$$

Similarly, at $\theta = \pi/2$, $X = \begin{pmatrix} 0 \\ 1 \end{pmatrix}$ and $X^{\perp} = \begin{pmatrix} -1 \\ 0 \end{pmatrix}$. Thus

$$A\begin{pmatrix} 0\\1 \end{pmatrix} = \mathcal{R}(\pi/2)\begin{pmatrix} 0\\1 \end{pmatrix} + \mathcal{T}(\pi/2)\begin{pmatrix} -1\\0 \end{pmatrix} = \begin{pmatrix} -\mathcal{T}(\pi/2)\\\mathcal{R}(\pi/2) \end{pmatrix}$$

Simultaneously, we know that

$$A\begin{pmatrix}1\\0\end{pmatrix} = \begin{pmatrix}a_{11}\\a_{21}\end{pmatrix}$$
, and $A\begin{pmatrix}0\\1\end{pmatrix} = \begin{pmatrix}a_{12}\\a_{22}\end{pmatrix}$.

The lemma follows.

The power of Corollary 2.2 is that System (2.1) can be uniquely defined either by the matrix A (i.e. the components $a_{11}, a_{12}, a_{21}, a_{22}$) or by the pair of functions \mathcal{R} and \mathcal{T} (i.e. the parameters m_R, m_T, p, θ_R).

Radial and tangential velocities of System (2.1). So far, we have focused on the vector field AX and its decomposition into radial and tangential components. With the next two corollaries, we reinterpret Theorem 2.1 in terms of the dynamics of System (2.1). On the unit circle, $\mathcal{R}(\theta)$ and $\mathcal{T}(\theta)$ give the radial and tangential velocities of solutions of System (2.1), respectively. This is very powerful: throughout the rest of the paper we exploit the radial structure of linear systems to study reactivity in all of \mathbb{R}^2 through the single variable functions $\mathcal{R}(\theta)$ and $\mathcal{T}(\theta)$.

COROLLARY 2.3. Given System (2.1) and a point $X = \begin{pmatrix} r\cos\theta\\r\sin\theta \end{pmatrix} \in \mathbb{R}^2$, the radial and angular velocities at X are given by

$$\frac{dr}{dt} = r\mathcal{R}(\theta)$$
$$\frac{d\theta}{dt} = \mathcal{T}(\theta)$$

and the tangential velocity is given by $r\mathcal{T}(\theta)$.

Proof. By Theorem 2.1, the vector field AX on the right side of System (2.1) has the form

$$\frac{dX}{dt} = \mathcal{R}(\theta)X + \mathcal{T}(\theta)X^{\perp} = r\mathcal{R}(\theta) \begin{pmatrix} \cos \theta \\ \sin \theta \end{pmatrix} + r\mathcal{T}(\theta) \begin{pmatrix} -\sin \theta \\ \cos \theta \end{pmatrix}.$$

Simultaneously, the left side of the equation can be written in terms of the polar coordinates (r, θ) as

$$\frac{dX}{dt} = \frac{dr}{dt} \begin{pmatrix} \cos \theta \\ \sin \theta \end{pmatrix} + r \frac{d\theta}{dt} \begin{pmatrix} -\sin \theta \\ \cos \theta \end{pmatrix}.$$

The result follows.

Restricting our attention to the unit circle S^1 , Corollary 2.3 states that for r = 1, the radial and tangential velocities are given by

$$\frac{dr}{dt} = \mathcal{R}(\theta) \tag{2.10}$$

$$\frac{d\theta}{dt} = \mathcal{T}(\theta) \tag{2.11}$$

Sinusoidal properties of \mathcal{R} and \mathcal{T} . Figures 2 and 6 - 8 show the graphs of $\mathcal{R}(\theta)$ and $\mathcal{T}(\theta)$ for a variety of matrices A. The striking sinusoidal characteristics of \mathcal{R} and \mathcal{T} follow immediately from Equations (2.4) and (2.5), and are gathered together in Corollary 2.4, Definition 3.6 and Table 1.

COROLLARY 2.4. The functions $\mathcal{R}(\theta)$ and $\mathcal{T}(\theta)$ are sinusoidal with period π . They have the same amplitude, p, and are $\frac{\pi}{4}$ out of phase. The midlines of \mathcal{R} and \mathcal{T} are given by m_R and m_T respectively. The maxima of \mathcal{R} and \mathcal{T} occur at θ_R and θ_T , respectively, where θ_R is defined in Equation (2.9) and $\theta_T = \theta_R - \frac{\pi}{4} \in \mathbb{R} \pmod{\pi}$. The maximum and minimum values of \mathcal{R} and \mathcal{T} are given by:

$$\rho_{1} = \max_{\theta \in \mathbb{R}} \mathcal{R}(\theta) = \mathcal{R}(\theta_{R}) = m_{R} + p$$

$$\rho_{2} = \min_{\theta \in \mathbb{R}} \mathcal{R}(\theta) = \mathcal{R}\left(\theta_{R} \pm \frac{\pi}{2}\right) = m_{R} - p$$

$$\tau_{1} = \max_{\theta \in \mathbb{R}} \mathcal{T}(\theta) = \mathcal{T}\left(\theta_{T}\right) = m_{T} + p$$

$$\tau_{2} = \min_{\theta \in \mathbb{R}} \mathcal{T}(\theta) = \mathcal{T}\left(\theta_{T} \pm \frac{\pi}{2}\right) = m_{T} - p$$

Up to this point, we have primarily considered $\theta \in \mathbb{R} \pmod{2\pi}$ as we have restricted our attention to the unit circle $S^1 \subset \mathbb{R}^2$. However, Corollary 2.4 shows that the dynamics of System 2.1 are π -periodic when viewed in radial and tangential

components. This is another clear consequence of linearity since the vector field at a point -X is exactly opposite the vector field at X. We also saw this π -periodicity when θ_R was defined to be in $\mathbb{R} \pmod{\pi}$: $\mathcal{R}(\theta)$ has a unique maximum in $\mathbb{R} \pmod{\pi}$. For these reasons, we can consider $\theta \in \mathbb{R} \pmod{\pi}$ with the understanding that by studying \mathcal{R} and \mathcal{T} in $\mathbb{R} \pmod{\pi}$ we are also studying the dynamics on both S^1 and the whole of \mathbb{R}^2 .

3. Recasting reactivity and attenuation in terms of \mathcal{R} and \mathcal{T} . Now that we have direct access to the radial dynamics of System (2.1) through the sinusoidal function \mathcal{R} , reactivity and attenuation are easily recast as the maximum and minimum values of \mathcal{R} , respectively:

COROLLARY 3.1. System (2.1) has reactivity $\rho_1 = m_R + p$ and attenuation $\rho_2 = m_R - p$. Thus, System (2.1) is reactive if and only if $\rho_1 > 0$ and attenuates if and only if $\rho_2 < 0$.

Proof. By the definition of reactivity (1.3), Corollaries 2.3 and 2.4, and Equation 2.10, the reactivity of System (2.1) is given by

$$\max_{X_0 \neq 0} \left(\left. \frac{1}{r_0} \frac{dr}{dt} \right|_{t=0} \right) = \max_{X_0 \in S^1} \left(\left. \frac{dr}{dt} \right|_{t=0} \right) = \max_{\theta \in \mathbb{R}} \mathcal{R}(\theta) = \rho_1$$

Similarly, the attenuation of System (2.1) is given by

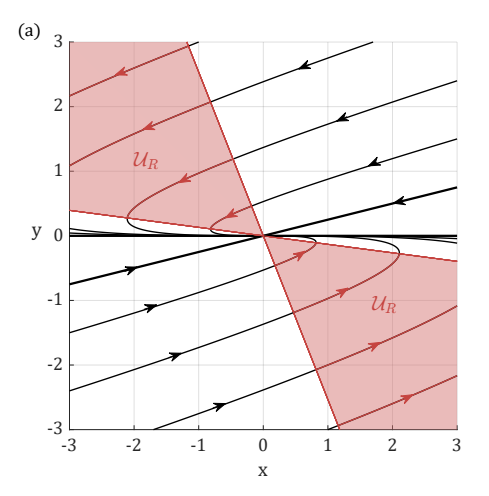
$$\min_{X_0 \neq 0} \left(\frac{1}{r_0} \frac{dr}{dt} \Big|_{t=0} \right) = \min_{\theta \in \mathbb{R}} \mathcal{R}(\theta) = \rho_2$$

Criteria for reactivity. From the definitions of reactivity and attenuation, it is clear that systems exhibiting asymptotic attraction must be attenuating and those exhibiting asymptotic repulsion must be reactive. Thus, systems with attracting equilibria are attenuating, systems with repelling equilibria are reactive, and systems with saddle equilibria are both reactive and attenuating. This observation is reestablished in the following corollaries which present immediate criteria, from the viewpoint afforded us by our radial and tangential decomposition, for System (2.1) to be reactive and attenuating. In particular, these criteria follow directly from the sinusoidal nature of the radial component \mathcal{R} and are given in terms of the of the midline, m_R , and amplitude, p, of \mathcal{R} .

Corollary 3.2. If $m_R > 0$, then System (2.1) is reactive. If $m_R < 0$, then System (2.1) attenuates.

Proof. This follows immediately from Corollaries 2.4 and 3.1, since $\rho_1 \geq m_R \geq \rho_2$. So if $m_R > 0$ then $\rho_1 > 0$ and System (2.1) is reactive. Similarly, if $m_R < 0$ then $\rho_2 < 0$ and System (2.1) attenuates.

Returning to our dynamical viewpoint, recall from Equation (2.6) that $m_R = \frac{1}{2} \text{tr}(A)$, where tr(A) denotes the trace of A. Equivalently, m_R is the average of the real parts of the eigenvalues of A. Thus, Corollary 3.2 says that repelling equilibria (and saddle equilibria whose stronger eigenvalue is positive) are reactive while attracting equilibria (and saddle equilibria whose stronger eigenvalue is negative) are attenuating. While these implications of Corollary 3.2 are expected, the criteria in Corollary 3.3 apply to the more subtle cases when System (2.1) is reactive despite m_R being negative or attenuating despite m_R being positive.



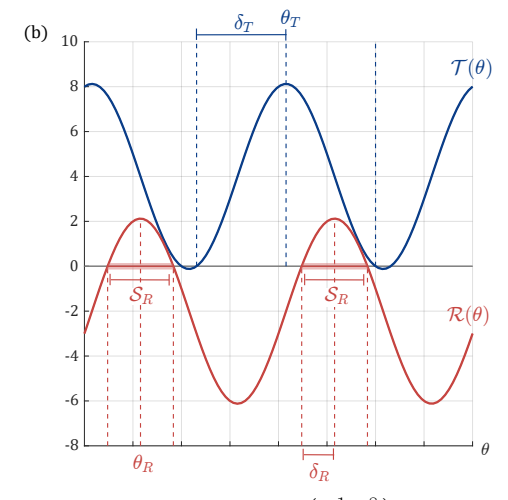


Fig. 3: (a) The phase portrait for the system with coefficient matrix $A = \begin{pmatrix} -1 & -8 \\ 0 & -3 \end{pmatrix}$ is shown with the reactive region \mathcal{U}_R highlighted in pink. (b) The corresponding radial and tangential components, \mathcal{R} and \mathcal{T} , are plotted in red and dark blue, respectively. The reactive set \mathcal{S}_R , where $\mathcal{R}(\theta) > 0$ is also shown. Notice the symmetry of the zeros of \mathcal{R} around θ_R with radius δ_R so that $\mathcal{S}_R = (\theta_R - \delta_R, \theta_R + \delta_R) \in \mathbb{R} \pmod{\pi}$. Similarly, the zeros of \mathcal{T} are symmetric around θ_T where δ_T is the angular distance between the maximum of \mathcal{T} and the zeros of \mathcal{T} .

COROLLARY 3.3. If $m_R \leq 0$ ($m_R \geq 0$), then System (2.1) is reactive (attenuating) if and only if $p > |m_R|$.

Proof. Corollary 3.3 follows immediately from Corollary 3.1.

While Corollary 3.3 is most interesting for the subtle cases of reactive attractors and attenuating repellers (specified in Corollary 3.4), it also holds for saddles. Thus, taken together Corollaries 3.2 and 3.3 affirm that saddles are always both reactive and attenuating based on these m_R and p criteria.

COROLLARY 3.4. If the origin is an attracting (repelling) equilibrium, then System (2.1) is reactive (attenuating) if and only if $p > |m_R|$.

Proof. Corollary 3.4 follows directly from Corollary 3.3, since $m_R \leq 0$ if the origin attracts, and $m_R \geq 0$ if the origin repels.

Reactive and attenuating regions. To further explore the concept of reactivity and its consequences for the transient dynamics of System (2.1), we use $\mathcal{R}(\theta)$ to decompose \mathbb{R}^2 into regions on which r is increasing (or decreasing) along trajectories. Figure 3 highlights this "reactive region" in red, illustrating the following definition.

DEFINITION 3.5. The reactive set, S_R , and attenuating set, S_C , of System (2.1) are defined by:

$$S_R = \{ \theta \in [0, 2\pi) \mid \mathcal{R}(\theta) > 0 \}, \quad S_C = \{ \theta \in [0, 2\pi) \mid \mathcal{R}(\theta) < 0 \}.$$

The reactive region, U_R , and attenuating region, U_C , are the cones defined by the reactive and attenuating sets, respectively:

$$\mathcal{U}_R = \left\{ (r, \theta) \in \mathbb{R}^2 \mid r > 0, \ \theta \in \mathcal{S}_R \right\}, \ \mathcal{U}_C = \left\{ (r, \theta) \in \mathbb{R}^2 \mid r > 0, \ \theta \in \mathcal{S}_C \right\}.$$

For $X \in \mathbb{R}^2$, we say System (2.1) is reactive at X if $X \in \mathcal{U}_R$.

The subscript C is chosen for the attenuating region to denote the contracting nature of attenuation.

If \mathcal{R} is not identically zero, then \mathcal{S}_R and \mathcal{S}_C share the same (possibly empty) boundary: $\partial \mathcal{S}_R = \partial \mathcal{S}_C = \{\theta \in S^1 \mid \mathcal{R}(\theta) = 0\}$, where ∂S denotes the boundary of set S. Similarly, $\partial \mathcal{U}_R = \partial \mathcal{U}_C = \{(r, \theta) \in \mathbb{R}^2 \mid \mathcal{R}(\theta) = 0\}$.

Since the boundary of these regions is given by the zeros of \mathcal{R} , we can use the symmetry of these zeros, a consequence of \mathcal{R} being sinusoidal, to further characterize $\partial \mathcal{S}_R$. In particular, if $\mathcal{R}(\theta)$ has any zeros, they are symmetrically located around θ_R (see Figure 3). Though unrelated to the boundary of the reactive region, a similar symmetry holds for the zeros of the tangential component $\mathcal{T}(\theta)$: if $\mathcal{T}(\theta)$ has any zeros, they are symmetrically located around θ_T . This symmetry in both \mathcal{R} and \mathcal{T} leads to the following definition.

DEFINITION 3.6. If $\mathcal{R}(\theta)$ has any zeroes, define $\delta_R > 0$ by

$$\mathcal{R}(\theta_R - \delta_R) = \mathcal{R}(\theta_R + \delta_R) = 0$$
and $\mathcal{R}(\theta) > 0$ on $(\theta_R - \delta_R, \theta_R + \delta_R) \subseteq \mathbb{R} \pmod{\pi}$

Similarly, if $\mathcal{T}(\theta)$ has any zeroes, define $\delta_T > 0$ by

$$\mathcal{T}(\theta_T - \delta_T) = \mathcal{T}(\theta_T + \delta_T) = 0$$
and $\mathcal{T}(\theta) > 0$ on $(\theta_T - \delta_T, \theta_T + \delta_T) \subseteq \mathbb{R} \pmod{\pi}$

With this new notation, we can now write $S_R = (\theta_R - \delta_R, \theta_R + \delta_R) \subset \mathbb{R} \pmod{\pi}$.

The reactive region is a useful tool for understanding the radial amplification of solutions of System 2.1. As illustrated in Figure 3, solutions of System 2.1 radially increase as they pass through the reactive region (marked in red), and decrease as they pass through the attenuating region. The angular movement of solutions through the reactive and attenuating regions is governed by $\mathcal{T}(\theta)$. In Figure 5, one can observe how different eigenvalue conditions affect the dynamics in the reactive and attenuating regions. In particular, if A has a positive real eigenvalue, the corresponding eigenvector lies in the reactive region, and if A has a negative real eigenvalue, the corresponding eigenvector lies in the attenuating region.

In Section 4 we describe how to read more of the features of the eigenvalues and eigenvectors of A from \mathcal{R} and \mathcal{T} . This will prepare us for defining analogous orthovalues and orthovectors in Section 5 from which we can harness features of the reactive region to better understand reactivity and transient dynamics.

4. Eigenvalues and eigenvectors through the lens of \mathcal{R} and \mathcal{T} . The following corollaries of Theorem 2.1 describe the way that the linear structure of System (2.1) is captured by \mathcal{R} and \mathcal{T} . In particular, Corollaries 4.1 and 4.2 link our new perspective to the traditional approach of studying linear systems via their eigenvalues and eigenvectors. Corollary 4.1 formalizes the fundamental observation that the zeros of \mathcal{T} capture the eigendirections of A (the vector field along these invariant radial directions necessarily has no angular component, see Figure 4). Corollary 4.2 shows how the eigenvalues can be calculated and interpreted in terms of the features of \mathcal{R} and \mathcal{T} . These results, along with a characterization of eigenvalue multiplicity in terms of \mathcal{R} and \mathcal{T} parameters, are summarized in Corollary 4.3.

COROLLARY 4.1. The vector $V = \begin{pmatrix} \cos \theta \\ \sin \theta \end{pmatrix} \in S^1$ is an eigenvector of A with corresponding eigenvalue $\mathcal{R}(\theta)$ if and only if $\mathcal{T}(\theta) = 0$.

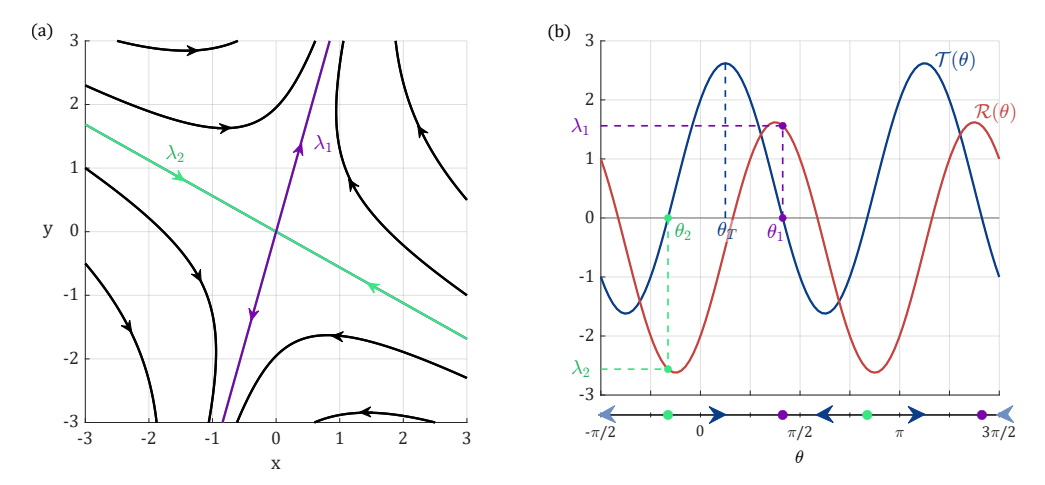


Fig. 4: (a) The phase portrait for the system with coefficient matrix $A = \binom{-2}{2} \binom{1}{1}$ is shown. The origin is a saddle whose eigenvectors are highlighted in dark purple (repelling direction) and in light green (attracting direction). The associated eigenvalues are $\lambda_1 = m_R + p_R > 0$ and $\lambda_2 = m_R - p_R < 0$ as given in Corollary 4.2. (b) The radial and tangential components, $\mathcal{R}(\theta)$ and $\mathcal{T}(\theta)$, are plotted in red and dark blue, respectively. Notice the eigenvectors in (a) correspond to the angles θ_1 and θ_2 in (b) and the eigenvalues λ_1 and λ_2 equal $\mathcal{R}(\theta_1)$ and $\mathcal{R}(\theta_2)$, respectively. Below the axes, we show the phase line of angular dynamics (Equation (2.11)) which highlights how trajectories move towards the repelling eigendirection (dark purple) in their long-term behavior (Corollary 4.4).

Proof. By Equation (2.3),

$$\mathcal{T}(\theta) = 0 \iff AV = \mathcal{R}(\theta)V + \mathcal{T}(\theta)V^{\perp} = \mathcal{R}(\theta)V$$

and the corollary follows.

In Definition 3.6, we observed that when \mathcal{T} has zeros, they are located symmetrically at $\theta_T \pm \delta_T$. Now we see that these angles correspond to the eigendirections of A. Corollary 4.1 also tells us that $\mathcal{R}(\theta_T \pm \delta_T)$ correspond to the eigenvalues of A. For consistency, we always write $\lambda_1 \geq \lambda_2$. Therefore, because of the direction of the $\pi/4$ phase shift between \mathcal{R} and \mathcal{T} , $\lambda_1 = \mathcal{R}(\theta_T + \delta_T)$ and $\lambda_2 = \mathcal{R}(\theta_T - \delta_T)$ (see Figure 4). This leads to the following notational convention.

NOTATION. If A has two distinct real eigenvectors, we let

$$\theta_1 = \theta_T + \delta_T \in \mathbb{R} \pmod{\pi}$$
 and $\theta_2 = \theta_T - \delta_T \in \mathbb{R} \pmod{\pi}$ (4.1)

denote the eigenvector angles so that $\lambda_i = \mathcal{R}(\theta_i)$ and $\lambda_1 \geq \lambda_2$.

In Section 6, we will develop tools from which we can easily calculate δ_T in terms of the features of \mathcal{R} and \mathcal{T} . In the meantime, we can apply the usual characteristic polynomial calculation to find the eigenvalues in terms of \mathcal{R} and \mathcal{T} by using the version of A given in Corollary 2.2.

Corollary 4.2. The eigenvalues of A are $\lambda_{1,2} = m_R \pm p_R$ where p_R is given by

$$p_R = \sqrt{p^2 - m_T^2} = \sqrt{-\tau_1 \tau_2} \tag{4.2}$$

and τ_1 and τ_2 are the maximum and minimum angular velocities as in Corollary 2.4 and Figure 2.

Proof. Writing A in terms of $\mathcal{R}(0)$, $\mathcal{T}(0)$, $\mathcal{R}(\pi/2)$ and $\mathcal{T}(\pi/2)$ as in Corollary 2.4, the trace and determinant of A are given by

$$tr(A) = 2 m_R$$
 and $det(A) = m_R^2 + m_T^2 - p^2$.

Using these to compute the roots of the characteristic polynomial yields

$$\lambda_{1,2} = m_R \pm \sqrt{p^2 - m_T^2}$$

$$= m_R \pm \sqrt{-(m_T + p)(m_T - p)} = m_R \pm \sqrt{-\tau_1 \tau_2}.$$

$$(4.3)$$

This calculation gives us a way to compute both real and complex eigenvalues in terms of \mathcal{R} and \mathcal{T} features. In the case of real eigenvalues, λ_1 and λ_2 are symmetric around the midline m_R . This is expected since $\mathcal{R}(\theta_T) = m_R$ and $\lambda_{1,2} = \mathcal{R}(\theta_T \mp \delta_T)$. In the case of complex eigenvalues, the real part is the average radial velocity m_R while the imaginary part, $\sqrt{\tau_1\tau_2}$, is the geometric mean of the maximum and minimum angular velocities. We discuss the dynamical significance of this after Corollary 4.4.

Equation (4.3) illuminates an important criteria for real vs complex eigenvalues: if $p^2 \geq m_T^2$, then p_R is real, but if $p^2 < m_T^2$, then p_R is imaginary. This same criteria is also clear when considering how many zeros \mathcal{T} must have within one period: \mathcal{T} only crosses the θ -axis if $|m_T| \leq p$. This is summarized in the following corollary.

Corollary 4.3.

- (i) $p > |m_T| \iff \mathcal{T}$ has two distinct zeroes in $\mathbb{R} \pmod{\pi} \iff A$ has distinct real eigenvalues $\lambda_{1,2} = \mathcal{R}(\theta_{1,2}) = m_R \pm p_R = m_R \pm \sqrt{-\tau_1 \tau_2}$.
- (ii) $p < |m_T| \iff \mathcal{T}$ has no zeroes $\iff A$ has a complex eigenvalue pair $\lambda_{1,2} = m_R \pm p_R = m_R \pm i\sqrt{\tau_1\tau_2}$.
- (iii) $p = |m_T| = 0 \iff \mathcal{T} \equiv 0 \iff every \ vector \ is \ an \ eigenvector, \ and \ A \ has$ the single real eigenvalue $\lambda = m_R$ with algebraic and geometric multiplicity 2.
- (iv) $p = |m_T| \neq 0 \iff \mathcal{T}$ has a unique zero in $\mathbb{R} \pmod{\pi} \iff A$ has the single real eigenvalue $\lambda = m_R$ with algebraic multiplicity 2 and geometric multiplicity 1.

Proof. Using the notation introduced in equation (4.1), Corollary 4.3 follows directly from Corollaries 4.1 and 4.2 and from Definition 3.6.

Figure 5 illustrates cases (i), (ii), and (iv) by looking at a series of matrices in which p is held constant while m_T is decreased in each subsequent system. An example of case (iii) is illustrated in Figure 6(a).

Eigenvectors and dynamics of the angular velocity. Returning to the dynamical viewpoint, note that the decomposition of System (2.1) into radial and tangential components has partially decoupled the dynamics, so that Equation (2.11) is an autonomous one-dimensional ODE for the angular dynamics. In Corollary 4.4 we identify the attracting equilibrium of the angular dynamics. This reveals the well known result that if A has distinct real eigenvalues, then the trajectories of System (2.1) converge to the eigendirection associated with the largest eigenvalue (e.g. the weak stable eigendirection when the origin attracts, the unstable eigendirection when the origin is a saddle, and the strong unstable eigendirection when the origin repels.)

COROLLARY 4.4. Eigenvectors of A correspond to equilibria of Equation (2.11). In the case when there are two distinct equilibria on $\mathbb{R} \pmod{\pi}$, the equilibrium θ_1

corresponding to eigenvalue $\mathcal{R}(\theta_1) = m_R + p_R$ attracts the angular dynamics, while the equilibrium θ_2 corresponding to eigenvalue $\mathcal{R}(\theta_2) = m_R - p_R$ repels the angular dynamics.

Proof. By Corollary 4.1, eigenvectors of A correspond to zeroes of \mathcal{T} , and hence to equilibria of Equation (2.11). In the case when \mathcal{T} has two distinct zeroes on $[0,\pi)$, we can determine the stability of the two corresponding equilibria by checking the sign of $\mathcal{T}'(\theta_1)$ and $\mathcal{T}'(\theta_2)$. Notice that because of the relationship between the sinusoidal structure of \mathcal{R} and \mathcal{T} , $\mathcal{T}'(\theta) = -2(\mathcal{R}(\theta) - m_R)$. This ensures that if $\mathcal{R}(\theta_1) > m_R > \mathcal{R}(\theta_2)$, then $\mathcal{T}'(\theta_1) < 0 < \mathcal{T}'(\theta_2)$, and the corollary follows. See Figure 4.

If \mathcal{T} has no zeros, then the angular dynamics has no equilibrium and solutions always move counter-clockwise (if $\mathcal{T} > 0$) or clockwise (if $\mathcal{T} < 0$). In this case,

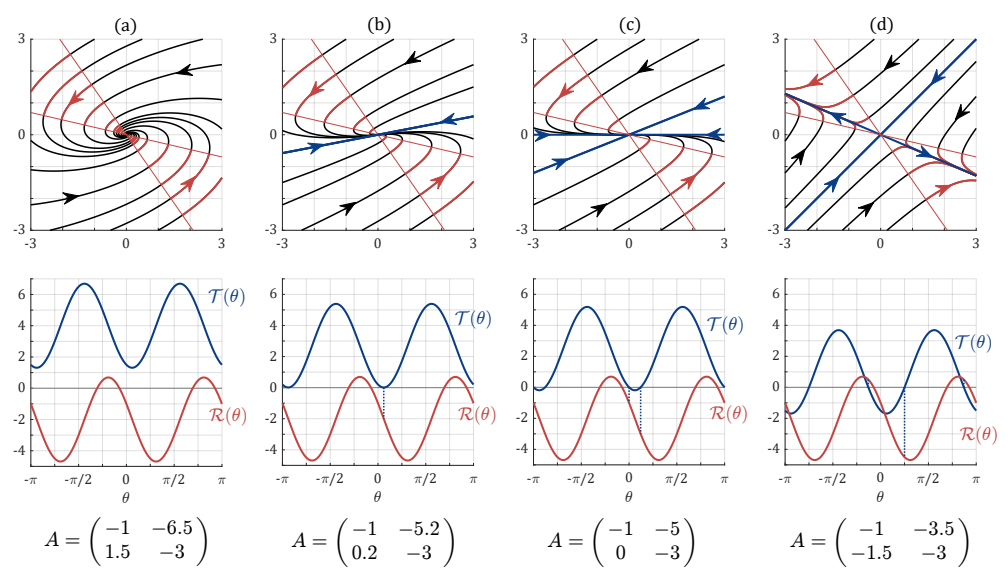


Fig. 5: We show the phase portraits and graphs of $\mathcal R$ and $\mathcal T$ associated with the four linear ODEs indicated by the coefficient matrices in the third row. All four of these systems have same radial component $\mathcal{R}(\theta)$ (that is, p, m_R , and θ_R remain unchanged). The difference between these systems is that m_T , the midline of \mathcal{T} , is shifted downward in each subsequent system to give rise to four qualitatively different the behaviors in the dynamics. (a) In the first system, $m_T = 4 > p$, and by Corollary 4.3, since \mathcal{T} has no zeros, there are no real eigenvalues. Dynamically, trajectories always rotate counter-clockwise and spiral inward since m_R is negative. However, since the reactivity is positive $\rho_1 = m_R + p > 0$, the systems is a reactive spiral sink. (b) When m_T is shifted down precisely so that $m_T = p$, \mathcal{T} has exactly one root and a single repeated real eigenvector emerges. Dynamically, every trajectory that is not on the eigenline exhibits counter-clockwise rotation toward the repeated eigenvector as it approaches the origin asymptotically. Along the way, these trajectories exhibit transient reactive behavior as they pass through the reactive region where $\mathcal{R}(\theta) > 0$. (c) When m_T is shifted down further so that $m_T < p$, the system has two real eigenvectors with two distinct eigenvalues $\lambda_{1,2} = m_R \pm p_R$. Since \mathcal{T} just barely passes below the θ -axis, the eigenvectors are quite close together $(p_R \text{ is small})$ and the system has a reactive attracting node. (d) When m_T is shifted down even further, the roots of \mathcal{T} get farther apart so that one root passes into the reactive region. This means that the larger eigenvalue $\lambda_1 = m_R + p_R$ becomes positive and the system exhibits saddle behavior.

by Corollaries 4.2 and 4.3, A has complex eigenvalues $\lambda_{1,2} = m_R \pm i\sqrt{\tau_1\tau_2}$. Accordingly, solutions to System (2.1) are a linear combination of $e^{m_R t}\cos(\sqrt{\tau_1\tau_2}t)$ and $e^{m_R t}\sin(\sqrt{\tau_1\tau_2}t)$. Therefore, all solutions have angular period $T=2\pi/\sqrt{\tau_1\tau_2}$, and the average angular speed over time with which solutions move either clockwise or counterclockwise is equal to $2\pi/T=\sqrt{\tau_1\tau_2}$, the geometric mean of the maximum and minimum \mathcal{T} values.

Symmetric attractors are non-reactive. We have seen how the radial and tangential framework illuminates eigenvalues and eigenvectors, and in particular, how the dynamics of the one-dimensional angular subsystem tell us about the asymptotic behavior System (2.1). In Section 5, we will take an analogous view of the reactive region by defining orthovalues and orthovectors. Before we do this, we consider the implications of Corollary 4.1 on the existence of reactivity when $m_T = 0$. Corollary 4.5 begins by recovering the well known result that symmetric matrices have real eigenvalues and orthogonal eigenvectors. See Figure 6.

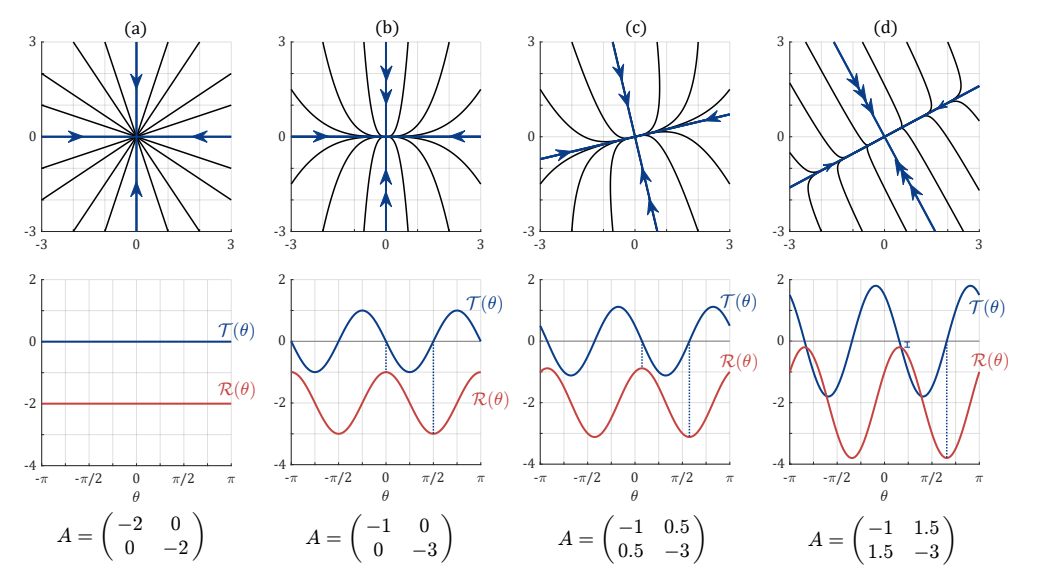


Fig. 6: We show the phase portraits and the graphs of \mathcal{R} and \mathcal{T} associated with the four linear ODEs indicated by the coefficient matrices in the third row. All four of these systems have symmetric coefficient matrices and showcase the equivalent features described in Corollary 4.5. (a) In this system, $\mathcal{T}(\theta)$ and $\mathcal{R}(\theta)$ are constant and $\mathcal{T}(\theta)$ is always equal to zero. Therefore every vector is an eigenvector with eigenvalue equal to $\mathcal{R}(\theta) \equiv -2$. (b) Like the matrix in (a), this coefficient matrix is diagonal and has eigenvectors at the axes. We can see this in the radial and tangential framework since $\mathcal{T}(0) = \mathcal{T}(\pi/2) = 0$. (c) While keeping the diagonal entries the same, we increase the off-diagonal elements of the coefficient matrix. This has the effect of slightly increasing the amplitude p and shifting the maximum θ_R of \mathcal{R} slightly to the right. The matrix is still symmetric, so $m_T = 0$ and the eigenvectors are still orthogonal though they have been rotated away from the coordinate axes. (d) By increasing the off-diagonal entries further, we significantly increase the amplitude p as well as further rotating the orthogonal eigenvectors (increasing θ_R). Notice that though m_R is the same as in (b) and (c), the largest eigenvalue, $\rho_1 = m_R + p$, has gotten quite close to zero, while the stronger negative eigenvalue $\rho_2 = m_R - p$ is much larger in magnitude. In the phase portrait, this can be seen as a strong attraction parallel to the $\theta_2 = \theta_R - \pi/2$ eigendirection before weak asymptotic attraction to the origin along the $\theta_1 = \theta_R$ eigendirection.

COROLLARY 4.5. If $\mathcal{T} \not\equiv 0$, the following statements are equivalent:

- (i) A is symmetric
- (ii) $m_T = 0$
- (iii) The zeroes of \mathcal{T} lie on the midline of \mathcal{T}
- (iv) A has orthogonal eigenvectors
- (v) A has real eigenvalues ρ_1 and ρ_2 (as defined in Corollary 2.4)
- (vi) A has eigenvectors V_1 and V_2 at angles θ_R and $\theta_R \pm \frac{\pi}{2}$ respectively.

Proof. $(i) \Leftrightarrow (ii)$ follows immediately from Equation (2.7)

- $(ii) \Leftrightarrow (iii)$ follows immediately from Equation (2.5)
- $(iii) \Leftrightarrow (iv)$ Since \mathcal{T} has period π , the zeroes of \mathcal{T} lie on the midline of \mathcal{T} if and only if they are angle $\frac{\pi}{2}$ apart, and the result follows from Corollary 4.1.
- $(iii) \Leftrightarrow (v)$ The $\frac{\pi}{4}$ phase shift between \mathcal{T} and \mathcal{R} ensures that \mathcal{R} reaches its maximum and minimum values, ρ_1 and ρ_2 respectively, exactly when \mathcal{T} is at its midline, and the result follows from Corollary 4.1.

 $(v) \Leftrightarrow (vi)$ follows from Corollaries 2.4 and 4.1

Corollaries 4.1 and 4.5 are statements about the eigenstructure of matrix A. Changing to a dynamical viewpoint, we re-interpret the results in terms of stability and reactivity properties of the equilibrium of System (2.1). Corollary 4.6 can, of course, be proven from the solutions of System (2.1). Here, we show how it follows directly from the properties of \mathcal{R} and \mathcal{T} .

COROLLARY 4.6. Given System (2.1), if A has orthogonal eigenvectors, then the origin is neither a reactive attractor nor an attenuating repeller.

Proof. By Corollary 4.5, A has eigenvalues ρ_1 and ρ_2 . If System (2.1) is reactive, then, by Corollary 3.1, the reactivity $\rho_1 > 0$, and so 0 is not an attractor. Similarly, if System (2.1) is attenuating, then the attenuation $\rho_2 < 0$, and 0 is not a repeller. \square

Taken together, Corollaries 4.5 and 4.6 show that if A is symmetric, then System (2.1) has neither a reactive attractor nor an attenuating repeller. By contrast, in Section 7 we show that any disjoint non-orthogonal pair of vectors can be the eigenvectors of a reactive attractor (and of an attenuating repeller).

5. Reactivity through the lens of orthovalues and orthovectors. In Section 3 we defined the reactive and attenuating regions \mathcal{U}_R and \mathcal{U}_C , respectively: cones bounded by the angles ϕ at which $\mathcal{R} = 0$. When $\mathcal{R}(\phi) = 0$, then, by Theorem 2.1, if $V = r \begin{pmatrix} \cos \phi \\ \sin \phi \end{pmatrix}$ then AV is orthogonal to V, thereby inspiring the following definition which establishes orthovectors and orthovalues as analogous to eigenvectors and eigenvalues. In the corollary that immediately follows, we prove that the orthovectors of A are always the boundaries of the reactive and attenuation regions and vice versa.

Definition 5.1. We call $V \in \mathbb{R}^2$ an orthovector of A with corresponding orthovalue μ if $AV = \mu V^{\perp}$.

COROLLARY 5.2. The vector $V = \begin{pmatrix} \cos \phi \\ \sin \phi \end{pmatrix} \in S^1$ is an orthovector of A with corresponding orthovalue $\mathcal{T}(\phi)$ if and only if $\mathcal{R}(\phi) = 0$.

Proof. The proof of Corollary 5.2 is analogous to that of Corollary 4.1: by Equation (2.3),

$$\mathcal{R}(\phi) = 0 \iff AV = \mathcal{R}(\phi)V + \mathcal{T}(\phi)V^{\perp} = \mathcal{T}(\phi)V^{\perp}$$

and the corollary follows.

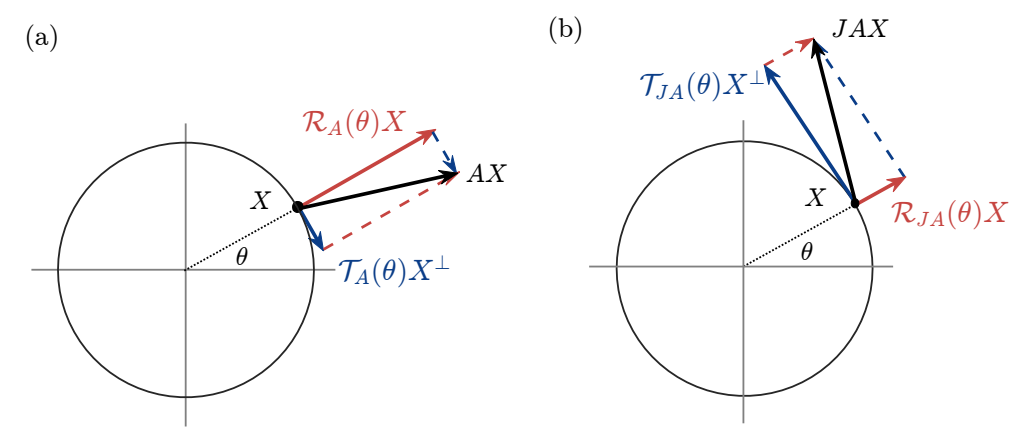


Fig. 7: The radial and tangential decompositions of the vector fields AX and JAX are depicted in (a) and (b), respectively. When the vector field given by AX is rotated counterclockwise by the matrix J, the components $\mathcal{R}_A(\theta)X$ and $\mathcal{T}_A(\theta)X^{\perp}$ are also rotated counterclockwise. The radial component $\mathcal{R}_{JA}(\theta)X$ of the new rotated vector field given by JAX is equal to the rotation of what was tangential component of AX: $\mathcal{R}_{JA}(\theta)X = J(\mathcal{T}_A(\theta)X^{\perp})$. Similarly, the tangential component $\mathcal{T}_{JA}(\theta)X^{\perp}$ of the new rotated vector field is equal to the rotation of of what was the radial component of AX: $\mathcal{T}_{JA}(\theta)X^{\perp} = J(\mathcal{R}_A(\theta)X)$. This geometric intuition is at the heart of Lemma 5.3.

Recall from Definition 3.6 that when \mathcal{R} has zeros they are located symmetrically at $\theta_R \pm \delta_R$. Just as we established eigenvector angles in section 4, we can now use Corollary 5.2 and Definition 3.6 to establish a standard notation for orthovector angles as the important boundaries of the reactive and attenuating sets, \mathcal{S}_R and \mathcal{S}_C , respectively.

NOTATION. If A has two distinct real orthovectors, we let

$$\phi_1 = \theta_R - \delta_R \quad and \quad \phi_2 = \theta_R + \delta_R$$
 (5.1)

denote the orthovector angles so that $S_R = (\phi_1, \phi_2) \subset \mathbb{R} \pmod{\pi}$ and $S_C = (\phi_2, \phi_1) \subset \mathbb{R} \pmod{\pi}$.

Correspondence between \mathcal{R} and \mathcal{T} via J. The connection between eigenvectors and orthovectors that is drawn by the analogous Corollaries 4.1 and 5.2 is a nod to the complementary relationship between the radial and tangential features of System (2.1). As illustrated in Figure 7, when the vector field is rotated by $\pi/2$, radial and tangential dynamics exchange places (up to appropriate sign correction). Lemma 5.3 formalizes this observation, and Corollary 5.4 shows how this correspondence allows us to calculate orthovalues and orthovectors as eigenvalues and eigenvectors of the rotated system.

LEMMA 5.3. Given a real 2×2 matrix A, and rotation matrix J as defined in Equation (2.2),

$$\mathcal{R}_{IA}(\theta) = -\mathcal{T}_A(\theta) \quad and \quad \mathcal{T}_{IA}(\theta) = \mathcal{R}_A(\theta)$$
 (5.2)

where the subscripts denote which system the radial and tangential components describe.

Proof. For any $X \in \mathbb{R}$, by Theorem 2.1,

$$(JA)X = \mathcal{R}_{JA}(\theta)X + \mathcal{T}_{JA}(\theta)X^{\perp}.$$

But we also have

$$J(AX) = J(\mathcal{R}_A(\theta)X + \mathcal{T}_A(\theta)X^{\perp})$$

= $\mathcal{R}_A(\theta)JX + \mathcal{T}_A(\theta)J(JX)$
= $\mathcal{R}_A(\theta)X^{\perp} - \mathcal{T}_A(\theta)X$,

since $J^2 = -I$. So, equating the coefficients of X and X^{\perp} , the result follows.

Corollary 5.4. $V \in \mathbb{R}^2$ is an orthovector of A with corresponding orthovalue μ if and only if V is an eigenvector of $J^{-1}A$ with corresponding eigenvalue μ .

Proof. $V \in \mathbb{R}^2$ is an eigenvector of $J^{-1}A$ with corresponding eigenvalue μ if and only if

$$J^{-1}AV = \mu V \iff AV = \mu JV = \mu V^{\perp}$$

and the result follows.

COROLLARY 5.5. The orthovalues of A are $\mu_{1,2} = m_T \pm p_T$ where p_T is given by

$$p_T = \sqrt{p^2 - m_R^2} = \sqrt{-\rho_1 \rho_2}$$

Proof. The proof follows directly from Lemma 5.3 and Corollaries 5.4 and 4.2. \square

Orthogonal orthovectors balance reactivity and attenuation. Just as orthogonal eigenvectors present a special case in Section 4 (Corollaries 4.5 and 4.6), orthogonal orthovectors can have significant implications for the dynamics of System 2.1. In Corollary 5.6, we present a list of equivalent conditions, before further discussing the resulting dynamics.

COROLLARY 5.6. If $\mathcal{R} \not\equiv 0$, the following statements are equivalent:

- (i) tr(A) = 0
- (ii) $m_R = 0$
- (iii) The zeroes of \mathcal{R} lie on the midline of \mathcal{R}
- (iv) A has orthogonal orthovectors
- (v) A has real orthovalues τ_1 and τ_2 (as defined in Corollary 2.4)
- (vi) A has orthovalues τ_1 and τ_2 with corresponding orthovectors V_1 and V_2 at angles $\theta_R \frac{\pi}{4}$ and $\theta_R + \frac{\pi}{4}$, respectively.

Proof. The proof of Corollary 5.6 is analogous to that of Corollary 4.5, with the roles of \mathcal{R} and \mathcal{T} interchanged.

Taking the dynamical point of view, if tr(A) = 0, then A has orthogonal orthovectors, so the reactive and attenuating regions of System (2.1) divide \mathbb{R}^2 equally into right-angled cones. Figure 8(b) shows a center in which the equal division of \mathbb{R}^2 into reactive and attenuating regions yields an equal balance of reactivity and attenuation, thereby leading to periodic orbits. By contrast, Figure 9 shows a series of attractors in which the reactive region grows as the reactivity increases, but the orthovectors never become quite orthogonal because both eigenvalues are negative, and hence their average, m_R , is negative.

Corollary 5.7 uses the intuition of balancing radial growth and radial decay to show that systems with orthogonal orthovectors must therefore either have a center equilibrium or have a saddle with symmetric attracting and repelling behavior.

COROLLARY 5.7. Given System (2.1), if $m_R = 0$ and $\mathcal{T} \not\equiv 0$, then the origin is a center if and only if \mathcal{T} is single signed, and a symmetric saddle (in the sense that the eigenvalues have equal magnitude) otherwise.

Proof. By Corollary 5.6, $m_R = 0 \Leftrightarrow \operatorname{tr}(A) = 0$, so the eigenvalues of A are given by $\pm 2\sqrt{\det(A)}$, where $\det(A)$ denotes the determinant of A. Thus:

 $\mathcal{T} \not\equiv 0$ is single signed $\Leftrightarrow \mathcal{T}$ has no zeroes

- $\Leftrightarrow A$ has no real eigenvalues, by Corollary 4.1
- $\Leftrightarrow A$ has imaginary eigenvalues $\pm \lambda i$, where $\lambda = \sqrt{-\det(A)}$

 \Leftrightarrow the origin is a center,

and similarly:

$$\mathcal{T} \not\equiv 0$$
 not single signed $\Leftrightarrow A$ has real eigenvalues $\pm \lambda$, where $\lambda = \sqrt{\det(A)}$ \Leftrightarrow the origin is a symmetric saddle.

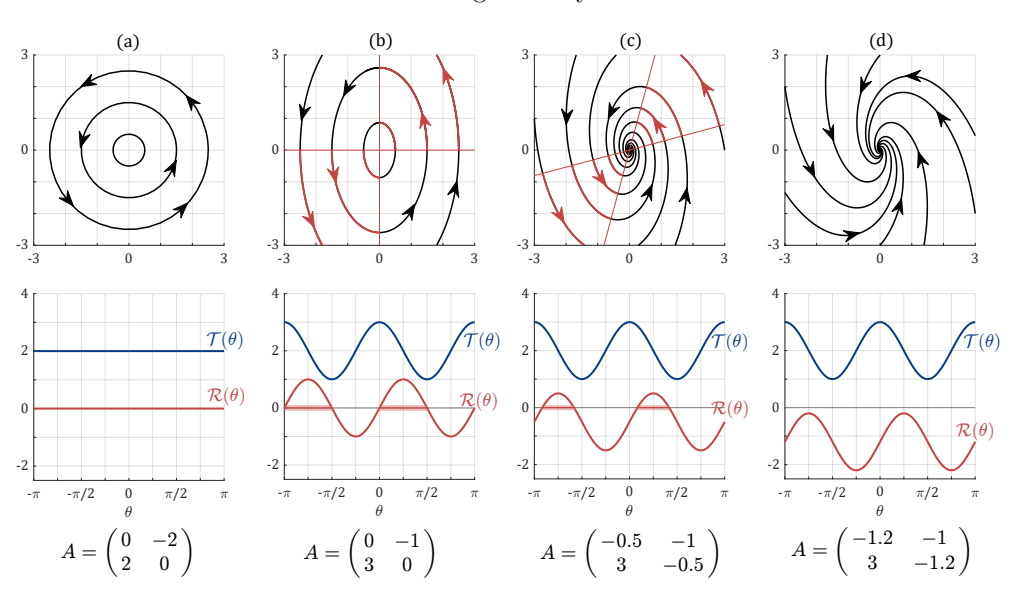


Fig. 8: We show the phase portraits and graphs of \mathcal{R} and \mathcal{T} associated with the four linear ODEs indicated by the coefficient matrices in the third row. (a) When p=0, both \mathcal{R} and \mathcal{T} are constant. Figure 6(a) illustrated the dynamics when $\mathcal{T} \equiv m_T \equiv 0$. Here, we see that when $\mathcal{R} \equiv m_R \equiv 0$, solutions to the differential equation exhibit pure rotation with a fixed radius and therefore have trajectories tracing out concentric circles. (b) When $m_R=0$ and $p \neq 0$, the orthovectors are orthogonal as in Corollary 5.6 and 5.7. Since \mathcal{T} is always positive in this system, the origin is a center: trajectories always rotate counter-clockwise and the equal balance of radial growth and radial decay ensures periodic oribts. (c) With $m_R < 0$, the orthovectors are no longer orthogonal. The radial decay outweighs the radial growth and the origin becomes a reactive spiral sink. (d) When $m_R < 0$ is shifted far enough, the system is no longer reactive $(\rho_1 < 0)$. Solution trajectories always exhibit radial decay and rotation in a counterclockwise direction, so the origin is a non-reactive spiral sink.

Ruling out reactivity. Corollary 4.3 presented a full characterization of how the radial and tangential features of (2.1) determine the asymptotic behavior of the system. Extending the analogy between eigenvectors and orthovectors, a similar result characterizes the possible transient dynamics of System (2.1).

Corollary 5.8.

- (i) $p > |m_R| \iff \mathcal{R}$ has two distinct zeros in $\mathbb{R} \pmod{\pi} \iff \mathcal{U}_R$ and \mathcal{U}_C both exist and are non-trivial.
- (ii) $p < |m_R| \iff \mathcal{R}$ has no zeros $\iff \rho_1$ and ρ_2 are either both positive or both negative.
- (iii) $p = |m_R| = 0 \iff \mathcal{R} \equiv 0 \iff \text{every vector is an orthovector with single } real \text{ orthovalue } \mu = m_T.$
- (iv) $p = |m_R| \neq 0 \iff \mathcal{R} \text{ has a unique zero in } \mathbb{R} \pmod{\pi} \iff \mathcal{S}_R = \{\theta_R\} \text{ for } m_R < 0 \text{ or } \mathcal{S}_C = \{\theta_R + \pi_2\} = \{\theta_R \pi/2\} \text{ for } m_R > 0.$

Proof. Corollary 5.8 follows from Theorem 2.1, Corollaries 3.1, 5.2 and 5.5, and Definitions 3.5 and 3.6. \Box

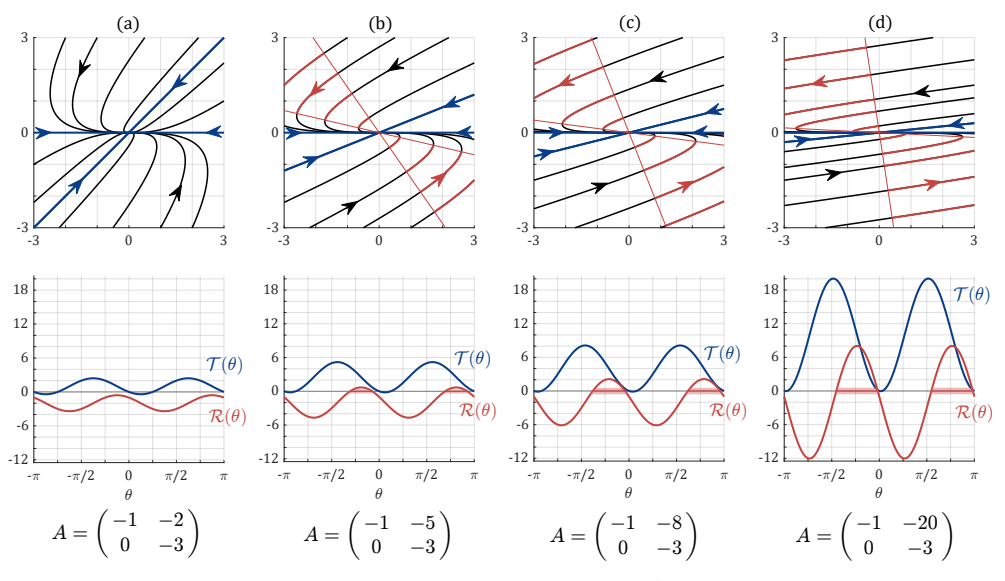


Fig. 9: We show the phase portraits and graphs of \mathcal{R} and \mathcal{T} associated with the four linear ODEs indicated by the coefficient matrices in the third row. In all four examples, the midlines m_T and m_R and the phase shift θ_R are held constant. The difference between these systems is that the amplitude p is stretched in each subsequent system to produce increasingly more extreme dynamics: eigenvectors get closer together (δ_T shrinks), eigenvalues become more unbalanced (p_R grows), and the reactivity ρ_1 grows to becomes positive, after which the reactive region (measured by δ_R) continues to grow. It is important to observe that though the eigenvectors get closer together in each subsequent system, the increase in reactivity is not caused by the proximity of the eigenvectors. Instead, the growth of reactivity and the growth reactive region are correlated with the squishing of the eigenvectors and the stretching of the eigenvalues because of the amplitude p which controls the magnitudes of both the radial and tangential components of the vector field. In Section 6, we find an explicit formula to describe this correlated relationship (see Corollary 6.6).

Cross-reference: The system in (b) is the same as in Figure 5(c). The system in (c) is the same as in Figures 1 and 3. The system in (b) is also used later in Figure 10 to illustrate the four standard matrix forms introduced in Section 6.

Parameter	Description	Notes
m_R	Midline of \mathcal{R}	
m_T	Midline of \mathcal{T}	
p	Amplitude of \mathcal{R} and \mathcal{T}	
θ_R	Location of maximum of \mathcal{R}	
θ_T	Location of maximum of \mathcal{T}	$\theta_T = \theta_R - \pi/4$
ρ_1	Reactivity, maximum of \mathcal{R}	$\rho_1 = m_R + p$
ρ_2	Attenuation, minimum of \mathcal{R}	$\rho_2 = m_R - p$
$ au_1$	Maximum of \mathcal{T}	$\tau_1 = m_T + p$
$ au_2$	Minimum of \mathcal{T}	$\tau_2 = m_T - p$
δ_R	Reactivity radius	$\mathcal{R}(\theta) > 0 \text{ on } (\theta_R - \delta_R, \theta_R + \delta_R)$
δ_T	Eigenvector separation radius	$\mathcal{T}(\theta) > 0 \text{ on } (\theta_T - \delta_T, \theta_T + \delta_T)$
θ_1, θ_2	Eigenvector angles	$\theta_1 = (\theta_T + \delta_T), \ \theta_2 = (\theta_T - \delta_T)$
$\lambda_1 \ge \lambda_2$	Eigenvalues	$\lambda_1 = \mathcal{R}(\theta_1), \ \lambda_2 = \mathcal{R}(\theta_2)$
p_R	Eigenvalue separation radius	$\lambda_1 = m_R + p_R, \ \lambda_2 = m_R - p_R$
ϕ_1, ϕ_2	Orthovector angles	$\phi_1 = (\theta_R - \delta_R), \ \phi_2 = (\theta_R + \delta_R)$
$\mu_1 \ge \mu_2$	Orthovalues	$\mu_1 = \mathcal{T}(\phi_1), \mu_2 = \mathcal{T}(\phi_2)$
p_T	Orthovalue separation radius	$\mu_1 = m_T + p_T, \mu_2 = m_T - p_T$

Table 1: Within the text, these definitions are found in Theorem 2.1, Corollary 2.4, Definition 3.6, Equation 4.1, Corollary 4.2, Equation 5.1, and Corollary 5.5. Additionally, methods to compute δ_R and δ_T are later presented in Corollary 6.6. The geometric meaning of many of these values is illustrated in Figures 2, 3, and 4.

Dynamically, case (i) in Corollary 5.8 corresponds to the three types of systems addressed in Corollary 3.3: reactive attractors, attenuating repellers, or saddles. Systems that satisfy case (ii) exhibit transient dynamics that are either always attracting or always repelling. Case (iii) describes systems with circular centers: every trajectory exhibits perfectly circular movement with uniform angular velocity m_T (see Figure 8(a)). Case (iv) characterizes systems that have repeated orthovectors and thus corresponds to the marginal transient dynamics that delineate either reactive attractors from nonreactive attractors or attenuating repellers from non-attenuating repellers. Though case (iv) is not explicitly depicted in our figures, this marginal case implicitly exists in Figure 8 between (c) and (d) as m_R is decreased and in Figure 9 between (a) and (b) as p is increased. In the special case that $m_T = 0$, (iv) also corresponds to systems that have one zero eigenvalue.

Not only, as Corollary 5.8 shows, does the concept of orthvectors allow us to more fully characterize the types of behaviors that are possible in linear systems, it also gives us a means of easily calculating important features of the transient dynamics and the language to describe relevant characteristics of the reactive region. Both the location of orthovectors relative to eigenvectors and the size and sign of orthovalues paint a picture for when a system experiences reactivity, to what extent, and in what way solution trajectories traverse the reactive region. In Section 6 we will rely on the explicit parallel between eigenvectors and orthovectors to develop four standard matrix types that leverage important features of our radial and tangential decomposition. In Section 7 we will use both the orthvectors and the orthovalues to calculate the extent to which transient repulsion (or attraction) can accumulate in asymptotically attracting (or repelling) linear systems.

6. Standard matrix forms for analyzing transient dynamics. It is standard practice to analyze the dynamics of System (2.1) via the Jordan canonical form. If, for example, A has distinct real eigenvectors, this involves conjugating by a coordinate change matrix M, so that $M^{-1}AM$ is diagonal. However, a diagonal matrix has orthogonal eigenvectors, and hence, by Corollary 4.6, the diagonalized system $\frac{dX}{dt} = (M^{-1}AM)X$ can never admit a reactive attractor nor an attenuating repeller. In other words, while the Jordan canonical form preserves eigenvalues and thereby captures the long-term asymptotic stability of System (2.1), it does not preserve eigenvector separation, and therefore fails to capture the transient dynamics of reactivity and attenuation.

One arena where this plays a significant role is in the analysis of linear nonautonomous dynamics where understanding time-dependent fluctuations of the eigenvalues (e.g. diagonalization) is insufficient to understand cumulative behavior (e.g. through transient effects). Josić and Rosenbaum address this difficulty in [7] where they utilize two standard matrices that fix transient features.

Motivated by [7], in this section, we identify four alternatives to the Jordan canonical form that preserve properties of both transient and asymptotic dynamics. Similar to the process of diagonalization, a matrix A can be analyzed in one of these standard forms through a conjugation by a coordinate change matrix M, however we restrict this transformation to rotation around the origin. Each of these matrix forms highlights a different aspect of the dynamics of System (2.1) by orienting (rotating) either the reactive region or the eigenvectors conveniently relative to the coordinate axes.

First we use \mathcal{R} and \mathcal{T} to define the four standard forms, and describe how they clarify the dynamics. Then in Theorem 6.2 we show how easy it is to write down these standard forms, for a given matrix A, in terms of the characteristics m_R , m_T and p of \mathcal{R} and \mathcal{T} , and the eigenvalues and orthovalues of A.

Definition 6.1. The real-valued 2×2 matrix A is in

- (i) \mathcal{R} -centered form if $\mathcal{R}_A(0) = \rho_1$, so \mathcal{R}_A attains its maximum at $\theta_R = 0$.
- (ii) \mathcal{T} -centered form if $\mathcal{T}_A(0) = \tau_1$, so \mathcal{T}_A attains its maximum at $\theta_T = 0$.
- (iii) \mathcal{R} -zeroed form if $\mathcal{R}_A(0) = 0$ and $\mathcal{R}'_A(0) \geq 0$, so \mathcal{R}_A attains its maximum at $\theta_R = \delta_R$.
- (iv) \mathcal{T} -zeroed form if $\mathcal{T}_A(0) = 0$ and $\mathcal{T}'_A(0) \geq 0$, so \mathcal{T}_A attains its maximum at $\theta_T = \delta_T$.

with $\rho_1, \tau_1, \theta_R, \theta_T, \delta_R$, and δ_T as in Table 1.

Dynamics of the standard matrix forms. If A is in \mathcal{R} -centered form, then $\theta_R = 0$, and the reactivity of System (2.1) is on the x-axis. If, moreover, A has real orthovalues, then the orthovector angles (zeros of \mathcal{R}_A) are $\pm \delta_R$ and the reactive region is centered on the x-axis as in Figure 10(a). If, by contrast, A is in \mathcal{R} -zeroed form, then it has orthovector angles at 0 and $2\delta_R$, so the x-axis forms one of the boundary lines of the reactive region. If the orthovalues are distinct ($\delta_R \neq 0$), then the condition $\mathcal{R}'_A(0) \geq 0$ ensures that the reactive region extends from the x-axis into the first and third quadrants as in Figure 10(c).

If A is in \mathcal{T} -centered form, then $\theta_T = 0$, and the maximum angular velocity of System (2.1) occurs on the x-axis. If, moreover, A has real eigenvalues, then the eigenvector angles (zeros of \mathcal{T}_A) are at $\pm \delta_T$ and the eigenvectors are symmetrically located relative the coordinate axes as in Figure 10(b). If, by contrast, A is in \mathcal{T} -zeroed form, then it has eigenvector angles at 0 and $2\delta_T$, so the x-axis is an eigenline. If the eigenvalues are distinct ($\delta_T \neq 0$), then the condition $\mathcal{T}'_A(0) \geq 0$ ensures that

 $\mathcal{T}_A > 0$ on $(0, 2\delta_T)$ and, in the angular dynamics, trajectories are directed away from the x-axis, as in Figure 10(d).

We may note that the \mathcal{T} -zeroed and \mathcal{R} -zeroed forms could have been chosen to have $\mathcal{T}'_A(0) \leq 0$ and $\mathcal{R}'_A(0) \leq 0$. We chose the convention so that the reactive region would be in the first quadrant. Notice that if $m_T > 0$, then this convention also provides us the intuition that radial growth starts on the x-axis and is accumulated through the first quadrant up until the second orthovector at $2\delta_R$. The resulting geometric intuition of the \mathcal{R} -zeroed form will be used in Section 7 to prove a sharp bound on the maximum amplification of System 2.1.

We now state Theorem 6.2 which designates the conjugations that take a matrix A to each of the four standard forms. We will henceforth denote the resulting four matrices and the radial and tangential components of their corresponding dynamics with the subscripts RC, TC, R0, and T0 for R-centered, T-centered, R-zeroed, and T-zeroed forms, respectively.

For the results and discussion that follow, we define M_{γ} to be the matrix representing (counter-clockwise) rotation by γ :

$$M_{\gamma} = \begin{pmatrix} \cos \gamma & -\sin \gamma \\ \sin \gamma & \cos \gamma \end{pmatrix} \tag{6.1}$$

THEOREM 6.2. Let A be a real 2×2 matrix with m_R , m_T , p, θ_R , θ_T , δ_R , δ_T , $\rho_{1,2}$, $\tau_{1,2}$, $\lambda_{1,2}$, and $\mu_{1,2}$ as in Table 1.

(i) If $\gamma = \theta_R$ and $A_{RC} = M_{\gamma}^{-1}AM_{\gamma}$, then A_{RC} is in \mathcal{R} -centered form, and

$$A_{RC} = \begin{pmatrix} \rho_1 & -m_T \\ m_T & \rho_2 \end{pmatrix}.$$

(ii) If $\gamma = \theta_T$ and $A_{TC} = M_{\gamma}^{-1} A M_{\gamma}$, then A_{TC} is in \mathcal{T} -centered form, and

$$A_{TC} = \begin{pmatrix} m_R & -\tau_2 \\ \tau_1 & m_R \end{pmatrix}.$$

(iii) When A has real orthovalues $\mu_1 > \mu_2$ with corresponding reactivity radius δ_R , if $\gamma = \theta_R - \delta_R$ and $A_{R0} = M_{\gamma}^{-1} A M_{\gamma}$, then A_{R0} is in \mathcal{R} -zeroed form, and

$$A_{R0} = \begin{pmatrix} 0 & -\mu_2 \\ \mu_1 & 2m_R \end{pmatrix}.$$

(iv) When A has real eigenvalues $\lambda_1 > \lambda_2$ with corresponding eigenvector separation radius δ_T , and $A_{T0} = M_{\gamma}^{-1} A M_{\gamma}$, then A_{T0} is in \mathcal{T} -zeroed form, and

$$A_{T0} = \begin{pmatrix} \lambda_2 & -2m_T \\ 0 & \lambda_1 \end{pmatrix}.$$

To our knowledge, the R-centered and R-zeroed forms have not been seen previously.

¹It is worth noting that matrices in \mathcal{T} -zeroed and \mathcal{T} -centered form (stated in Theorem 6.2 and in Table 2) are familiar examples in the reactivity literature. In particular, [1] uses an upper triangular matrix to illustrate the first example of reactivity. Though this example is not strictly in \mathcal{T} -zeroed form since $\mathcal{T}'(0) < 0$, upper triangular matrices which place an eigenvector on the x-axis have continued to be primary case studies for the presence of reactivity.

Similarly, \mathcal{T} -centered form has been seen previously in literature. [13] uses this form to illustrate that reactivity can get arbitrarily large for fixed eigenvalues, and [8] uses this form in a non-autonomously switching linear system to show that reactivity can lead to instability. The \mathcal{T} -centered matrix also mirrors the matrix form established in [7] to provide an alternative standard matrix to the upper-triangular matrix in the case of complex rather than real eigenvectors.

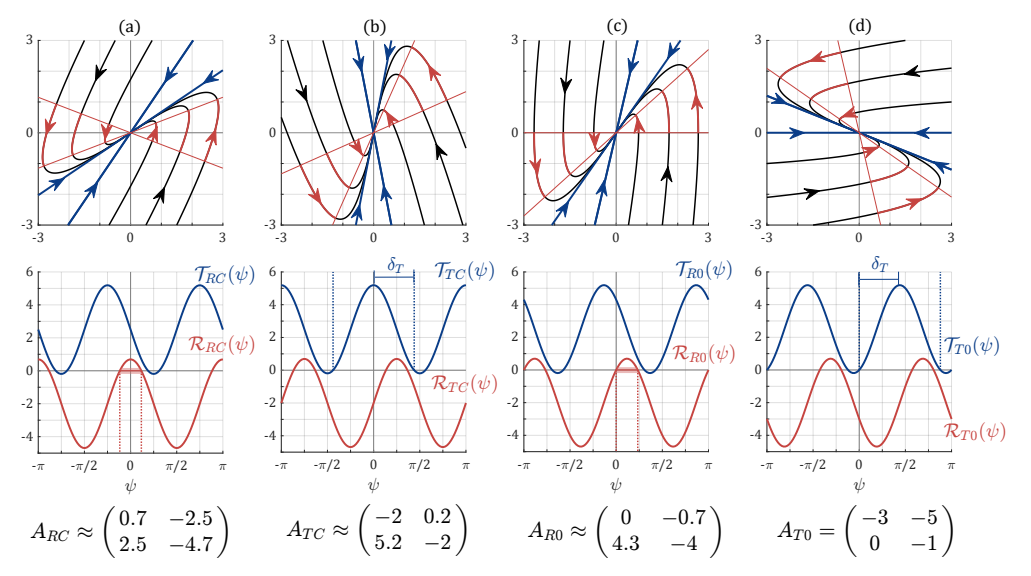


Fig. 10: The phase portraits and graphs of \mathcal{R} and \mathcal{T} associated with the four standard matrix forms of the system with coefficient matrix $A = \begin{pmatrix} -1 & -5 \\ 0 & -3 \end{pmatrix}$ is given in the same layout as Figures 6-8. The original system associated with A is shown in Figure 9(b). The horizontal axis for the graphs of \mathcal{R} and \mathcal{T} are given in terms of the new coordinate $\psi := \theta - \gamma$, as in Lemma 6.3, where γ is the rotation parameter as specified in Theorem 6.2 and Table 2. Notice how each of the transient and asymptotic features mentioned in Corollary 6.5 are equivalent across the four standard forms; the only features that change are the locations of the eigenvectors, orthovectors, and extrema of \mathcal{R} and \mathcal{T} , as stated in Lemma 6.4.

Table 2 summarizes these four standard forms of A, together with their associated \mathcal{R} and \mathcal{T} equations, eigenvector angles and eigenvalues (when real), orthovector angles and orthovalues (when real), and conjugation angle γ . Figure 10 shows examples of the standard forms and their corresponding dynamics for $A = \begin{pmatrix} -1 & -5 \\ 0 & -3 \end{pmatrix}$, of Figure 9(b).

Before proving Theorem 6.2, we will establish some important facts about conjugating by rotation including how to interpret this transformation in terms of \mathcal{R} and \mathcal{T} (Lemmas 6.3 and 6.4) and invariant properties of the transformation (Corollary 6.5).

Conjugation by rotation as a horizontal shift of \mathcal{R} and \mathcal{T} . Transforming the vector field AX using a conjugation by rotation of the matrix A creates a horizontal shift of the radial and tangential components in terms of the variable θ . Lemma 6.3 proves this fact from an algebraic perspective. Later we will turn again to a dynamics perspective and consider this conjugation by rotation as a coordinate change in System 2.1.

LEMMA 6.3. Given a real 2×2 matrix A, if $B = M_{\gamma}^{-1}AM_{\gamma}$, then

$$\mathcal{R}_B(\theta) = \mathcal{R}_A(\theta + \gamma) \text{ and } \mathcal{T}_B(\theta) = \mathcal{T}_A(\theta + \gamma).$$

Proof. If $X = \begin{pmatrix} r\cos\theta\\r\sin\theta \end{pmatrix}$, then rotation by γ gives $M_{\gamma}X = \begin{pmatrix} r\cos(\theta+\gamma)\\r\sin(\theta+\gamma) \end{pmatrix}$. Therefore, by Theorem 2.1,

$$A(M_{\gamma}X) = \mathcal{R}_{A}(\theta + \gamma)(M_{\gamma}X) + \mathcal{T}_{A}(\theta + \gamma)(M_{\gamma}X)^{\perp}$$

Since M_{γ} represents rotation around the origin, $(M_{\gamma}X)^{\perp} = M_{\gamma}X^{\perp}$. Thus

$$BX = M_{\gamma}^{-1}AM_{\gamma}X$$

$$= M_{\gamma}^{-1}(\mathcal{R}_{A}(\theta + \gamma)M_{\gamma}X + \mathcal{T}_{A}(\theta + \gamma)M_{\gamma}X^{\perp})$$

$$= \mathcal{R}_{A}(\theta + \gamma)M_{\gamma}^{-1}M_{\gamma}X + \mathcal{T}_{A}(\theta + \gamma)M_{\gamma}^{-1}M_{\gamma}X^{\perp}$$

$$= \mathcal{R}_{A}(\theta + \gamma)X + \mathcal{T}_{A}(\theta + \gamma)X^{\perp}$$

But, by Theorem 2.1, we also have

$$BX = \mathcal{R}_B(\theta)X + \mathcal{T}_B(\theta)X^{\perp}$$

and the lemma follows.

Because conjugation by rotation corresponds simply to a horizontal shift of the graphs of \mathcal{R} and \mathcal{T} , the vertical features of \mathcal{R} and \mathcal{T} , namely the midlines m_R and m_T and the amplitude p all remain unchanged. This preserves the transient dynamics such as the reactivity ρ_1 , the attenuation ρ_2 , and the radius of the reactive region δ_R , as well as the asymptotic dynamics (e.g. the eigenvalues λ_1 and λ_2).

Conjugation by rotation viewed as a coordinate change. Dynamically, if $B = M_{\gamma}^{-1}AM_{\gamma}$, the general solution of Y' = BY is given by $Y(t) = M_{\gamma}^{-1}X(t)$, where X(t) is the general solution of X' = AX. In other words, trajectories of X' = AX are rotated by $-\gamma$ radians around the origin to give trajectories of Y' = BY [14].

Geometrically, we can imagine picking up the phase portrait of X' = AX, rotating it by $-\gamma$ radians, and placing it back down again to give the phase portrait of Y' = BY. Alternatively, we can imagine changing coordinates by picking up the coordinate axes, rotating them counter-clockwise by γ , and placing them back down again.

This can be seen in Figure 10. In part (a), the system is in \mathcal{R} -centered form (rotated from the original by $\gamma_{RC} = \theta_R$). In part (b), the system is in \mathcal{T} -centered form (rotated from the original by $\gamma_{TC} = \theta_T = \theta_R - \pi/4$). Because $\gamma_{TC} = \gamma_{RC} - \pi/4$, we can think of the transition from part (a) to part (b) as a conjugation by rotation of $\gamma = -\pi/4$ radians. If we "pick-up" the phase portrait in part (a), rotate it counterclockwise by $\pi/4$ radians, and place back down, we get the phase portrait in part (b). Similarly, if we "pick-up" the coordinate axes in part (a), rotate them clockwise by $\pi/4$ radians, and place them back down, we would end up with the same dynamics as in part (b), viewed from a slightly different angle; notably, the new "y"-axis would be located in the acute angle between the eigenvectors as in part (b).

To connect the geometric intuition of this change of coordinates to our \mathcal{R} and \mathcal{T} framework, we consider this transformation in terms of the polar coordinates. Recall that if $B = M_{\gamma}^{-1}AM_{\gamma}$, then the dynamics of Y' = BY are given by the dynamics of X' = AX through the change of coordinates $Y := M_{\gamma}^{-1}X$. In polar coordinates, M_{γ}^{-1} takes (r,θ) to $(r,\theta-\gamma)$. Therefore, conjugation by rotation corresponds to a change of coordinates from (r,θ) to (r,ψ) , where $\psi = \theta - \gamma$. Then, by Lemma 6.3, $\mathcal{R}_B(\psi) = \mathcal{R}_A(\theta)$ and $\mathcal{T}_B(\psi) = \mathcal{T}_A(\theta)$. This is illustrated, for example, in Figure 10(a) where the system has been put into \mathcal{R} -centered form through a rotation by $\gamma_{RC} = \theta_R$. We observe that $\mathcal{R}_{RC}(0) = \mathcal{R}_A(\theta_R) = \rho_1$ and $\mathcal{T}_{RC}(0) = \mathcal{T}_A(\theta_R) = m_T$ where $\psi = \theta - \gamma_{RC}$.

Figure 10(a) can also help us to geometrically understand the horizontal shift in Lemma 6.3. Imagine \mathcal{R}_A and \mathcal{T}_A being picked up and dragged horizontally until the maximum of \mathcal{R}_A has been relocated from $\theta = \theta_R$ to $\psi = 0$. From this geometric

intuition, it is clear that all the features of \mathcal{R} and \mathcal{T} are, thereby, linearly translated horizontally by γ , and the only feature of the dynamics of System (2.1) that is altered by a conjugation by rotation is the angle, relative to the x-axis at which the dynamics occur. Lemma 6.4 and Corollary 6.5 of Lemma 6.3 establish these observations and allow us to prove Theorem 6.2.

LEMMA 6.4. Given a real 2×2 matrix A, if $B = M_{\gamma}^{-1}AM_{\gamma}$, then

- (i) If A has eigenvector angles θ_1 , θ_2 , then B has eigenvector angles $\theta_1 \gamma$, $\theta_2 \gamma$.
- (ii) If A has orthovector angles ϕ_1 , ϕ_2 , then B has orthovector angles $\phi_1 \gamma$, $\phi_2 \gamma$.
- (iii) If A achieves its reactivity ρ_1 (maximum of \mathcal{R}_A) at angle θ_R , then B achieves its reactivity ρ_1 at angle $\theta_R \gamma$.

Proof. Part (i). By Corollary 4.1, A has an eigenvector located at angle θ_i if and only if $\mathcal{T}_A(\theta_i) = 0$. Thus, $\mathcal{T}_B(\theta_i - \gamma) = \mathcal{T}_A(\theta_i) = 0$ and B has an eigenvector located at angle $\theta_i - \gamma$. Parts (ii) and (iii) follow similarly from Definition 5.1 and Corollary 2.4, respectively.

COROLLARY 6.5. The following properties of a real 2×2 matrix A are invariant under conjugation by rotation:

- (i) the midlines, m_R and m_T , of R and T, respectively
- (ii) the amplitude, p, of R and T
- (iii) the reactivity, ρ_1 (maximum of \mathcal{R}), and attenuation, ρ_2 (minimum of \mathcal{R})
- (iv) the maximum, τ_1 , and minimum, τ_2 , of \mathcal{T}
- (v) the eigenvalues, λ_1 and λ_2 , of A
- (vi) the angle $2\delta_T$ between the eigenvectors
- (vii) the orthovalues, μ_1 and μ_2 , of A
- (viii) the radius δ_R of the reactive region

Proof of Theorem 6.2 and Table 2. With the understanding of conjugation by rotation M_{γ} afforded us by Lemmas 6.3, 6.4, and Corollary 6.5, we are now ready to prove Theorem 6.2. Along the way we will also prove the facts presented in Table 2 such as the location for the maximum of \mathcal{T} denoted ψ_R , the location for the maximum of \mathcal{T} denoted ψ_T , the simplified forms for the radial and tangential components, and the location of the eigenvectors and orthovectors in each of the four standard matrix forms.

Proof of part (i). \mathcal{R} -centered form. If $\gamma = -\theta_R$, then conjugation by M_{γ} corresponds to a change in polar coordinates from (r, θ) to (r, ψ) , where $\psi = \theta - \theta_R$. Thus, by Corollary 6.4, A_{RC} achieves its reactivity, ρ_1 , at angle $\psi_R = 0$, and, by Definition 6.1, A_{RC} is in \mathcal{R} -centered form.

To find \mathcal{R}_{RC} and \mathcal{T}_{RC} in the new ψ coordinate, we apply Theorem 2.1, noting that $\psi_R = 0$, and that, by Corollary 6.5, m_T , m_R and p are all invariant under conjugation by M_{γ} , so can be calculated directly from A. Thus,

$$\mathcal{R}_{RC}(\psi) = m_R + p\cos(2(\psi - 0)) = m_R + p\cos(2\psi)$$
 (6.2)

$$\mathcal{T}_{RC}(\psi) = m_T - p\sin(2(\psi - 0)) = m_T - p\sin(2\psi) \tag{6.3}$$

To find A_{RC} , we apply Lemma 2.2 to Equations (6.2) and (6.3), noting that, by Corollary 6.5 again, the reactivity $\rho_1 = m_R + p$ and attenuation $\rho_2 = m_R - p$ are

invariant under conjugation by M_{γ} :

$$\begin{split} A_{RC} &= \begin{pmatrix} \mathcal{R}_{RC}(0) & -\mathcal{T}_{RC}(\pi/2) \\ \mathcal{T}_{RC}(0) & \mathcal{R}_{RC}(\pi/2) \end{pmatrix} = \begin{pmatrix} m_R + p\cos(0) & -m_T + p\sin(\pi) \\ m_T - p\sin(0) & m_R + p\cos(\pi) \end{pmatrix} \\ &= \begin{pmatrix} m_R + p & -m_T \\ m_T & m_R - p \end{pmatrix} = \begin{pmatrix} \rho_1 & -m_T \\ m_T & \rho_2 \end{pmatrix}. \end{split}$$

The proof of parts (ii)-(iv) are similar to that of part (i).

Proof of part (ii). \mathcal{T} -centered form. Recall that (r,θ) represents the original coordinates for System (2.1) with matrix A. We know from Corollary 2.4 that $\mathcal{T}_A(\theta)$ achieves its maximum value at $\theta_T = \theta_R - \pi/4$. Thus, under the change of coordinates from (r,θ) to (r,ψ) , where $\psi = \theta - \theta_T$, the maximum of \mathcal{T}_{TC} occurs at $\psi_T = 0$. So if $\gamma = -\theta_T$, then $A_{TC} = M_{\gamma}^{-1}AM_{\gamma}$ is in \mathcal{T} -centered form. Applying Theorem 2.1, and noting that, by Corollary 2.4, $\psi_T = 0 \Leftrightarrow \psi_R = \pi/4$, \mathcal{R}_{TC} and \mathcal{T}_{TC} in the new ψ coordinate are given by:

$$\mathcal{R}_{TC}(\psi) = m_R + p\cos(2\psi - \pi/2) = m_R + p\sin(2\psi)$$

 $\mathcal{T}_{TC}(\psi) = m_T - p\sin(2\psi - \pi/2) = m_T + p\cos(2\psi).$

Applying Lemma 2.2 again to find A_{TC} , and noting that, by Corollary 6.3, the maximum $\tau_1 = m_T + p$ and minimum $\tau_2 = m_T - p$ of \mathcal{T}_A are invariant under conjugation by M_{γ} , we have:

$$A_{TC} = \begin{pmatrix} \mathcal{R}_{TC}(0) & -\mathcal{T}_{TC}(\pi/2) \\ \mathcal{T}_{TC}(0) & \mathcal{R}_{TC}(\pi/2) \end{pmatrix} = \begin{pmatrix} m_R + p\sin(0) & -(m_T + p\cos(\pi)) \\ m_T + p\cos(0) & m_R + p\sin(\pi) \end{pmatrix}$$
$$= \begin{pmatrix} m_R & -(m_T - p) \\ m_T + p & m_R \end{pmatrix} = \begin{pmatrix} m_R & -\tau_2 \\ \tau_1 & m_R \end{pmatrix}.$$

Proof of part (iii). \mathcal{R} -zeroed form. We know, from the sinusoidal nature of \mathcal{R} , that if \mathcal{R}_A achieves its maximum at θ_R , then the orthovector angles (zeros of \mathcal{R}_A) are at $\theta_R \pm \delta_R$, and the reactive region is $(\theta_R - \delta_R, \theta_R + \delta_R)$. Thus, under the change of coordinates from (r, θ) to (r, ψ) , where $\psi = \theta - (\theta_R - \delta_R)$, the following are all true: the reactive region of \mathcal{R}_{R0} is $(0, 2\delta_R)$, $\mathcal{R}_{R0}(0) = 0$, the maximum of \mathcal{R}_{R0} occurs at $\psi_R = \delta_R$, and A_{R0} is in \mathcal{R} -zeroed form. Applying Theorem 2.1:

$$\mathcal{R}_{R0}(\psi) = m_R + p\cos(2(\psi - \delta_R))$$

$$\mathcal{T}_{R0}(\psi) = m_T - p\sin(2(\psi - \delta_R)).$$

Next we apply Lemma 2.2 to find A_{R0} . We can find $\mathcal{R}_{R0}(\pi/2)$ and $\mathcal{T}_{R0}(\pi/2)$ by noting that in \mathcal{R} -zeroed form $\psi = 0$ is the orthovector ($\mathcal{R}_{R0}(0) = 0$) associated with the larger orthovalue ($\mathcal{T}_{R0}(0) = \mu_1 = m_T + p_T$). (See Table 1 and Figures 3 and 10). It follows that

$$\mathcal{R}_{R0}(0) = m_R + p\cos(-2\delta_R) = 0$$
, so $p\cos(-2\delta_R) = -m_R$, and $\mathcal{R}_{R0}(\pi/2) = m_R + p\cos(\pi - 2\delta_R) = m_R - p\cos(-2\delta_R) = 2m_R$.

Similarly

$$\mathcal{T}_{R0}(0) = m_T - p\sin(-2\delta_R) = \mu_1 = m_T + p_T$$
, so $p\sin(-2\delta_R) = -p_T$, and $\mathcal{T}_{R0}(\pi/2) = m_T - p\sin(\pi - 2\delta_R) = m_T + p\sin(-2\delta_R) = m_T - p_T = \mu_2$.

Hence,

$$A_{R0} = \begin{pmatrix} \mathcal{R}_{R0}(0) & -\mathcal{T}_{R0}(\pi/2) \\ \mathcal{T}_{R0}(0) & \mathcal{R}_{R0}(\pi/2) \end{pmatrix} = \begin{pmatrix} 0 & -\mu_2 \\ \mu_1 & 2m_R \end{pmatrix}.$$

Proof of part (iv). \mathcal{T} -zeroed form. We know that if \mathcal{T}_A achieves its maximum at $\theta_T = \theta_R - \pi/4$, then the eigenvector angles (zeros of \mathcal{T}_A) are at $\theta_T \pm \delta_T$, and $\mathcal{T}(\theta) > 0$ on the interval $(\theta_T - \delta_T, \theta_T + \delta_T)$. Thus, under the change of coordinates from (r, θ) to (r, ψ) , where $\psi = \theta - (\theta_T - \delta_T)$, $\mathcal{T}_{T0}(0) = 0$, $\mathcal{T}_{T0} > 0$ on $(0, 2\delta_R)$, the maximum of \mathcal{T}_{T0} occurs at $\psi_T = \delta_T$, and A_{T0} is in \mathcal{T} -zeroed form. Applying Theorem 2.1, and noting that, by Corollary 2.4, $\psi_T = \delta_T \Leftrightarrow \psi_R = \delta_T + \pi/4$, yields:

$$\mathcal{R}_{T0}(\psi) = m_R + p\cos(2(\psi - \delta_T) - \pi/2) = m_R + p\sin(2(\psi - \delta_T))$$

$$\mathcal{T}_{T0}(\psi) = m_T - p\sin(2(\psi - \delta_T) - \pi/2) = m_T + p\cos(2(\psi - \delta_T)).$$

This time, to apply Lemma 2.2 to find A_{T0} , note that in \mathcal{T} -zeroed form, $\psi = 0$ is the eigenvector angle $(\mathcal{T}_{T0}(0) = 0)$ associated with the smallest eigenvalue, $\mathcal{R}_{T0}(0) = \lambda_2 = m_R - p_R$. (See Table 1 and Figures 4 and 10.) Therefore to calculate $\mathcal{T}_{T0}(\pi/2)$ and $\mathcal{R}_{T0}(\pi/2)$ we argue that

$$\mathcal{T}_{T0}(0) = m_T + p\cos(-2\delta_T) = 0$$
, so $p\cos(-2\delta_T) = -m_T$, and $\mathcal{T}_{T0}(\pi/2) = m_T + p\cos(\pi - 2\delta_T) = m_T - p\cos(-2\delta_R) = 2m_T$.

Similarly,

$$\mathcal{R}_{T0}(0) = m_R + p \sin(-2\delta_T) = \lambda_2 = m_R - p_R$$
, so $p \sin(-2\delta_T) = -p_R$, and $\mathcal{R}_{T0}(\pi/2) = m_R + p \sin(\pi - 2\delta_T) = m_R - p \sin(-2\delta_T) = m_T + p_R = \lambda_1$.

Hence.

$$A_{T0} = \begin{pmatrix} \mathcal{R}_{T0}(0) & -\mathcal{T}_{T0}(\pi/2) \\ \mathcal{T}_{T0}(0) & \mathcal{R}_{T0}(\pi/2) \end{pmatrix} = \begin{pmatrix} \lambda_2 & -2m_T \\ 0 & \lambda_1 \end{pmatrix}.$$

Calculating δ_R and δ_T . Among the important facts detailed in Theorem 6.2, the location of the orthovectors and eigenvectors (when real) in the \mathcal{R} -centered and \mathcal{T} -centered forms, give us easy ways to compute δ_R and δ_T respectively.

COROLLARY 6.6. Let A by any real, 2×2 matrix. If A has real orthovectors, then δ_R is given by the zeros of R_{RC} and the orthovalues $\mu_{1,2} = m_T \pm p_T$ so that

$$\cos(2\delta_R) = \frac{-m_R}{p} \quad and \quad \sin(2\delta_R) = \frac{p_T}{p}.$$
 (6.4)

Similarly, if A has real eigenvectors, then δ_T is given by the zeros of T_{TC} and the eigenvalues $\lambda_{1,2} = m_R \pm p_R$ so that

$$\cos(2\delta_T) = \frac{-m_T}{p} \quad and \quad \sin(2\delta_T) = \frac{p_R}{p}. \tag{6.5}$$

Moreover, the ratio between the eigenvector and eigenvalue separations and between the orthovector and orthovalue separations of system (2.1) are fixed by the amplitude p as follows:

$$p = \frac{p_R}{\sin(2\delta_T)} = \frac{p_T}{\sin(2\delta_R)} \tag{6.6}$$

	${\mathcal R} ext{-centered}\colon$	$\mathcal{T} ext{-centered}$:	${\mathcal R} ext{-zeroed}$:	$\mathcal{T} ext{-zeroed}$:
Matrix:	Matrix: $A_{RC} = \begin{pmatrix} \rho_1 & -m_T \\ m_T & \rho_2 \end{pmatrix}$	$A_{TC} = \begin{pmatrix} m_R & -\tau_2 \\ \tau_1 & m_R \end{pmatrix}$	$A_{R0} = \begin{pmatrix} 0 & -\mu_2 \\ \mu_1 & 2m_R \end{pmatrix}$	$A_{T0} = \begin{pmatrix} \lambda_2 & -2m_T \\ 0 & \lambda_1 \end{pmatrix}$
$\mathcal{R}(\psi) = \mathcal{T}(\psi) = \mathcal{T}(\psi)$	$m_R + p\cos(2\psi)$ $m_T - p\sin(2\psi)$	$m_R + p\sin(2\psi)$ $m_T + p\cos(2\psi)$	$m_R + p \cos(2(\psi - \delta_R))$ $m_T - p \sin(2(\psi - \delta_R))$	$m_R + p \sin(2(\psi - \delta_T))$ $m_T + p \cos(2(\psi - \delta_T))$
Phase shift:	$\psi_R = 0, \psi_T = -\frac{\pi}{4}$	$\psi_R = \frac{\pi}{4}, \psi_T = 0$	$\psi_R = \delta_R, \psi_T = \delta_R - \frac{\pi}{4}$	$\psi_R = \delta_T + \frac{\pi}{4}, \ \psi_T = \delta_T$
Horizontal shift:	$\gamma = \theta_R$	$\gamma = \theta_T = \theta_R - \pi/4$	$\gamma = \theta_R - \delta_R$	$\gamma = \theta_T - \delta_T$
Eigenvectors:	$rac{-\pi}{4}\pm\delta_T$	$\pm \delta_T$	$\delta_R - rac{\pi}{4} \pm \delta_T$	$0, 2\delta_T$
$\lambda_1 = m_R + p_R$ $\lambda_2 = m_R - p_R$	$\lambda_1 = \mathcal{R}_{RC}(\frac{-\pi}{4} + \delta_T)$ $\lambda_2 = \mathcal{R}_{RC}(\frac{-\pi}{4} - \delta_T)$	$\lambda_1 = \mathcal{R}_{TC}(+\delta_T)$ $\lambda_2 = \mathcal{R}_{TC}(-\delta_T)$	$\lambda_1 = \mathcal{R}_{R0} \left(\delta_R - \frac{\pi}{4} + \delta_T \right)$ $\lambda_2 = \mathcal{R}_{R0} \left(\delta_R - \frac{\pi}{4} - \delta_T \right)$	$\lambda_1 = \mathcal{R}_{T0}(2\delta_T)$ $\lambda_2 = \mathcal{R}_{T0}(0)$
Orthovectors:	$\pm \delta_R$	$rac{\pi}{4}\pm\delta_R$	$0, 2\delta_R$	$\delta_T + rac{\pi}{4} \pm \delta_R$
$\mu_1 = m_T + p_T$ $\mu_2 = m_T - p_T$	$\mu_1 = \mathcal{T}_{RC}(-\delta_R)$ $\mu_2 = \mathcal{T}_{RC}(+\delta_R)$	$\mu_1 = \mathcal{T}_{TC}(\frac{\pi}{4} - \delta_R)$ $\mu_2 = \mathcal{T}_{TC}(\frac{\pi}{4} + \delta_R)$	$\mu_1 = \mathcal{T}_{R0}(0)$ $\mu_2 = \mathcal{T}_{R0}(2\delta_R)$	$\mu_1 = \mathcal{T}_{T0}(\delta_T + \frac{\pi}{4} - \delta_R)$ $\mu_2 = \mathcal{T}_{T0}(\delta_T + \frac{\pi}{4} + \delta_R)$

and \mathcal{T} , ψ_R and ψ_T , respectively. The fourth row specifies the angle γ by which the system is rotated to be in given standard form (Thm. 6.2). The remaining rows describe the eigenvectors and eigenvalues (if they are real valued) and the orthovectors and orthovalues (if they are real valued). The parameters m_R , m_T , p, n_1 , p, n_2 , δ_T , and δ_R are invariant across all four standard forms (see Cor. 6.5 and Table 1). Table 2: Each column characterizes one of the four standard matrix forms (Def. 6.1). The first two rows specify the matrix form given by Thm. 6.2 and the corresponding $\mathcal R$ and $\mathcal T$ equations. The third row describes the phase shift of $\mathcal R$ and $\mathcal T$ described by the new locations of the maxima of $\mathcal R$

Proof. To calculate δ_R , we use Theorem 6.2 and Corollary 6.5 to assume, without loss of generality, that A is in \mathcal{R} -centered form wherein the orthovectors are centered and the zeros of \mathcal{R}_{RC} are thus located at $\pm \delta_R$. As in Table 2, $\mathcal{R}_{RC}(\delta_R) = m_R + p\cos(2\delta_R)$, yielding the first part of Equation (6.4). Since the orthovectors in \mathcal{R} -centered form are located at $\pm \delta_R$, the orthovalue $\mu_1 = m_T + p_T$ is given by $\mathcal{T}_{RC}(\delta_R) = m_T - p\sin(2\delta_R)$, yielding the second part of Equation (6.4).

Similarly, to calculate δ_T , we use \mathcal{T} -centered form wherein the eigenvectors are centered and the zeros of \mathcal{T}_{RC} are located at $\pm \delta_T$. As in Table 2, $\mathcal{T}_{TC}(\delta_T) = m_T + p\cos(2\delta_T)$, yielding the first part of Equation (6.5). Since the eigenvectors in \mathcal{T} -centered form are located at $\pm \delta_T$, the eigenvalue $\lambda_1 = m_R + p_R$ is given by $\mathcal{R}_{TC}(\delta_T) = m_R + p\sin(2\delta_T)$, yielding the second part of Equation (6.5).

Equation
$$(6.6)$$
 follows directly from Equations (6.4) and (6.5) .

Corollary 6.6 establishes a computable relationship between δ_R , m_R and p, and δ_T , m_T and p by using centered standard forms. It also establishes an explicit relationship between eigenvector separation δ_T and eigenvalue separation p_R and between orthovector separation δ_R and orthovalue separation p_T (see Figure 9). This give us multiple approaches for calculating δ_R and δ_T , and for relating them to other features of \mathcal{R} and \mathcal{T} . In particular, the amplitude p and midline m_T of \mathcal{T} are fully determined by the eigenvector separation angle δ_T and the eigenvalue separation radius p_R . Conversely, the amplitude p and the midline m_R of \mathcal{R} are fully determined by the radius of the reactive region δ_R and the orthovalue separation p_T .

As we will see later in the proofs of Lemma 7.2 and Corollary 7.6, the relationships established in Corollary 6.6 facilitate the navigation between overlapping geometric and algebraic intuitions and allow us to calculate and describe dynamics of interest fluidly. In the next section, we further show how this framework and the accompanying \mathcal{R} -focused standard forms inform our intuition and lead to a readily accessible understanding of transient reactivity and accumulated radial growth.

7. Reactivity is unbounded, but maximal amplification is bounded. Recall from the introduction that Neubert and Caswell [1] introduce the maximal (radial) amplification of perturbations to the origin in a reactive attracting system as follows:

DEFINITION 7.1. If System 2.1 has a reactive attractor at the origin, the maximal amplification, ρ_{max} , is the maximum factor by which a perturbation can be amplified before returning to the origin:

$$\rho_{max} = \max_{t_*>0} \left[\max_{X_0 \neq 0} \left(\frac{\|X(t_*)\|}{\|X_0\|} \right) \right] = \max_{t_*>0} \left[\max_{X_0 \neq 0} \left(\frac{r(t_*)}{r_0} \right) \right].$$

The amplification time, t_{max} , is the time required to achieve this maximal amplification:

 $\rho_{max} = \max_{X_0 \neq 0} \left(\frac{r(t_{max})}{r_0} \right).$

In Lemma 7.2, Theorems 7.3 and 7.4, below, we show that when System 2.1 has an attractor, the reactivity of the system (i.e. the maximal instantaneous rate of radial amplification) can be arbitrarily large, and is independent of the eigenvalues and eigenvectors of the system. By contrast, in Theorem 7.5 and Corollary 7.6 we show

that the maximum amplification of the system has simple upper bounds determined by the orthovector separation and eigenvector separation of A, respectively. Then, in Theorem 7.7, we calculate the maximal amplification exactly.

Reactivity is unbounded. Lemma 7.2 shows that the reactivity of System (2.1) is independent of both the eigenvector separation and the reactivity radius. Based on this lemma, Theorem 7.3 shows that a reactive attractor with any combination of real, negative eigenvalues can have any reactivity, while Theorem 7.4 shows that a reactive attractor with any non-parallel, non-orthogonal pair of eigenvectors can have any reactivity. In both cases, these results show that reactivity can be arbitrarily large. Analogous theorems hold, with similar proofs, for attenuating repellers.

LEMMA 7.2. Fix any $\delta_R \in (0, \pi/2), \delta_T \in [0, \pi/2), \text{ and } \rho \in \mathbb{R}^+$. The linear system (System 2.1) with coefficient matrix A given by

$$A = \frac{\rho}{1 - \cos(2\delta_R)} \begin{pmatrix} -\cos(2\delta_R) & 1 + \cos(2\delta_T) \\ 1 - \cos(2\delta_T) & -\cos(2\delta_R) \end{pmatrix}$$

has real eigenvalues and orthovalues, with the given eigenvector separation radius δ_T , reactivity radius δ_R , and reactivity ρ .

REMARK. The matrix A given in Lemma 7.2 is in \mathcal{T} -centered form. By Corollary 6.5, any conjugation of A by rotation will also have the same eigenvector separation radius, reactivity radius, and reactivity.

Before proving that A has the properties listed in Lemma 7.2, we note that we constructed A geometrically, by first constructing $\mathcal{R}(\theta)$ and $\mathcal{T}(\theta)$ and then applying Corollary 2.2 to recover the coefficients of the matrix A. To construct $\mathcal{R}(\theta)$ and $\mathcal{T}(\theta)$ in \mathcal{T} -centered form, we apply a vertical shift of $-\cos(2\delta_R)$ and $-\cos(2\delta_T)$ to the functions $\cos(2\theta)$ and $\sin(2\theta)$, respectively, to ensure that $\mathcal{R}(\frac{\pi}{4} \pm \delta_R) = 0$ and $\mathcal{T}(\pm \delta_T) = 0$. We then scale both functions by $p = \frac{\rho}{1-\cos(2\delta_R)}$ to ensure that $\mathcal{R}(\theta)$ has the desired maximum: $\mathcal{R}(\pi/4) = \rho$.

Proof. It is straightforward to check that A has real eigenvalues and orthovalues by Corollaries 4.3 and 5.8, since $|m_T| \le p$, and $|m_R| < p$. Then, by Corollary 6.6, the eigenvector separation radius is given by:

$$\frac{1}{2}\arccos\left(\frac{-m_T}{p}\right) = \frac{1}{2}\arccos\left(\frac{-(a_{21} - a_{12})}{\sqrt{(a_{11} - a_{22})^2 + (a_{12} + a_{21})^2}}\right)$$
$$= \frac{1}{2}\arccos\left(\frac{2\cos(2\delta_T)}{\sqrt{4}}\right)$$
$$= \delta_T$$

Similarly, the reactivity radius of System 2.1 is given by:

$$\frac{1}{2}\arccos\left(\frac{-m_R}{p}\right) = \frac{1}{2}\arccos\left(\frac{-(a_{11} + a_{22})}{\sqrt{(a_{11} - a_{22})^2 + (a_{12} + a_{21})^2}}\right)$$
$$= \frac{1}{2}\arccos\left(\frac{2\cos(2\delta_R)}{\sqrt{4}}\right)$$
$$= \delta_R$$

Finally, by Corollary 3.1, the reactivity of System 2.1 is given by:

$$m_R + p = \frac{1}{2}(a_{11} + a_{22}) + \frac{1}{2}\sqrt{(a_{11} - a_{22})^2 + (a_{12} + a_{21})^2}$$
$$= \frac{\rho}{1 - \cos(2\delta_R)} \left(-\cos(2\delta_R) + 1\right)$$
$$= \rho$$

THEOREM 7.3. Given any $\lambda_2 \leq \lambda_1 < 0$ and any $\rho > 0$, there is a real 2×2 coefficient matrix A for which System 2.1 has a reactive attractor with eigenvalues λ_1 and λ_2 and reactivity ρ .

Proof. By Corollaries 3.1, 4.3 and 6.6, δ_R is calculated by

$$\delta_R = \frac{1}{2} \arccos\left(\frac{-m_R}{p}\right)$$

where $m_R = \frac{1}{2}(\lambda_1 + \lambda_2) < 0$ and $p = \rho - m_R > 0$ so that $\delta_R \in (0, \pi/4)$. Similarly, by Corollary 6.6, δ_T satisfies

$$\sin(2\delta_T) = \frac{p_R}{p}$$

where $p_R = \lambda_1 - m_R \ge 0$. We can therefore choose

$$\delta_T = \frac{1}{2} \arcsin\left(\frac{p_R}{p}\right) \in [0, \pi/4).$$

Now we have δ_R, δ_T and ρ , so the result follows from Lemma 7.2.

Remark. Once again, the matrix A given by Lemma 7.2 in Theorem 7.3 is in \mathcal{T} -centered form, and by Corollary 6.5, any conjugation of A by rotation will also have the same eigenvalues and reactivity.

THEOREM 7.4. Given any non-zero, non-orthogonal, non-parallel pair of vectors $V_1, V_2 \in \mathbb{R}^2$ and any $\rho > 0$, there is a real 2×2 coefficient matrix B with eigenvectors V_1, V_2 , for which the corresponding system has a reactive attractor with reactivity ρ .

Proof. Let $\theta_1, \theta_2 \in [0, 2\pi)$ measure the angles from the $\theta = 0$ axis to V_1 and V_2 , respectively. Without loss of generality, assume the vectors V_1, V_2 are labeled so that $\theta_1 - \theta_2 \in (0, \pi)$. Now let $\delta_T = \frac{1}{2}(\theta_1 - \theta_2) \in (0, \pi/2)$, and choose $\delta_R \in (0, |\delta_T - \pi/4|)$. Note that δ_R is well-defined in $(0, \pi/4)$ since, by assumption the vectors V_1 and V_2 are non-orthogonal $(\delta_T \neq \pi/4)$.

We have δ_R, δ_T and ρ , so we can apply Lemma 7.2 to find a matrix A in \mathcal{T} -centered form, with eigenvectors at angles $\pm \delta_T$, real eigenvalues, reactivity radius δ_R and reactivity ρ .

To confirm that the eigenvalues of A are both negative, note that by Corollary 6.6, as a consequence of \mathcal{R} -centered and \mathcal{T} -centered form,

$$m_B = -p\cos(2\delta_B)$$
 and $p_B = p\sin(2\delta_T)$.

Therefore the largest eigenvalue, given by

$$m_R + p_R = -p(\cos(2\delta_R) - \sin(2\delta_T))$$

= $-p(\cos(2\delta_R) - \cos(2(\delta_T - \pi/4)).$

Since $\delta_R \in (0, |\delta_T - \pi/4|) \subseteq (0, \pi/4)$, $\delta_R < |\delta_T - \pi/4|$ implies that $\cos(2\delta_R)$ is larger than $\cos(2(\delta_T - \pi/4)) = \cos(2|\delta_T - \pi/4|)$. Therefore $m_R + p_R < 0$ and both eigenvalues are negative.

Finally, to place the eigenvectors at V_1 and V_2 , as desired, without changing the eigenvalues or the reactivity, we conjugate by the appropriate rotation. Specifically, let $B = M_{\gamma}^{-1} A M_{\gamma}$, where $\gamma = -\frac{1}{2}(\theta_1 + \theta_2)$. Then, by Lemma 6.3,

$$\mathcal{T}_B(\theta_1) = \mathcal{T}_A\left(\theta_1 - \frac{1}{2}(\theta_1 + \theta_2)\right) = \mathcal{T}_A\left(\frac{1}{2}\theta_1 - \frac{1}{2}\theta_2\right) = \mathcal{T}_A(\delta_T) = 0, \text{ and }$$

$$\mathcal{T}_B(\theta_2) = \mathcal{T}_A\left(\theta_2 - \frac{1}{2}(\theta_1 + \theta_2)\right) = \mathcal{T}_A\left(-\frac{1}{2}\theta_1 + \frac{1}{2}\theta_2\right) = \mathcal{T}_A(-\delta_T) = 0.$$

Thus System 2.1, with matrix B, has a reactive attractor with eigenvectors V_1 and V_2 and reactivity ρ .

Maximal Amplification is Bounded. In Theorem 7.5 and Corollary 7.6, we prove estimates on the upper bound of the maximum amplification ρ_{max} , showing that for a fixed reactivity radius δ_R or a fixed eigenvector separation radius δ_T , though the reactivity ρ is unbounded, the maximal accumulation of that reactive growth is bounded.

THEOREM 7.5. If System 2.1 has a reactive attractor at the origin, with reactivity radius $\delta_R \in (0, \pi/4)$, then the maximal amplification, ρ_{max} is bounded above by

$$\rho_{max} < \frac{1}{\cos(2\delta_R)} = -\frac{p}{m_R}.$$

Proof. The proof is encapsulated in Figure 11. Without loss of generality, assume that A is in \mathcal{R} -zeroed form, so, as in Table 2, the lines bounding the reactive region, which are associated with the orthovectors, are at $\theta = 0$ and $\theta = 2\delta_R$. The reactive region is given by $\theta \in (0, 2\delta_R) \cup (\pi, \pi + 2\delta_R)$. Trajectories experience radial amplification during their passage through the reactive region, and radial attenuation elsewhere. Since the origin is attracting, we know there is net attenuation, so the maximal amplification is achieved by exactly traversing a single component of the reactive region.

Consider the case $\mathcal{T} > 0$ on the reactive region (we know \mathcal{T} has no zeros on the reactive region since A has no positive eigenvalues). Then the orthovalues, $\mu_1 = \mathcal{T}(0)$ and $\mu_2 = \mathcal{T}(2\delta_R)$, are positive and correspond to counter clockwise motion through the reactive region. To fix ideas, consider the trajectory with initial condition $X_0 = (1,0)^T$ on the "entrance" boundary of the reactive region. This trajectory X(t) achieves maximal amplification at the point W, where it reaches the "exit" boundary of the reactive region at $\theta = 2\delta_R$. Thus $\rho_{max} = ||W||$, since $||X_0|| = 1$.

Since X(t) solves System 2.1, which we have assumed without loss of generality is in \mathcal{R} -zeroed form, the vector field is given by

$$\frac{dX}{dt} = AX = \begin{pmatrix} 0 & -\mu_2 \\ \mu_1 & 2m_R \end{pmatrix} \begin{pmatrix} x \\ y \end{pmatrix} = \begin{pmatrix} -\mu_2 y \\ \mu_1 x + 2m_R y \end{pmatrix}.$$

With this equation, we can see that $\frac{dX}{dt}\big|_{X=X_0} = (0,\mu_1)^T$ and points orthogonally into the reactive region (as expected since X_0 is an orthovector with orthovalue μ_1). As X(t) then traverses the reactive region, the first component of $\frac{dX}{dt}$ is negative (since y>0 and $\mu_2>0$). Hence, the x-coordinate of the point W is less than the x-coordinate of X_0 and W is closer to the origin along the line $\theta=2\delta_R$ than the point

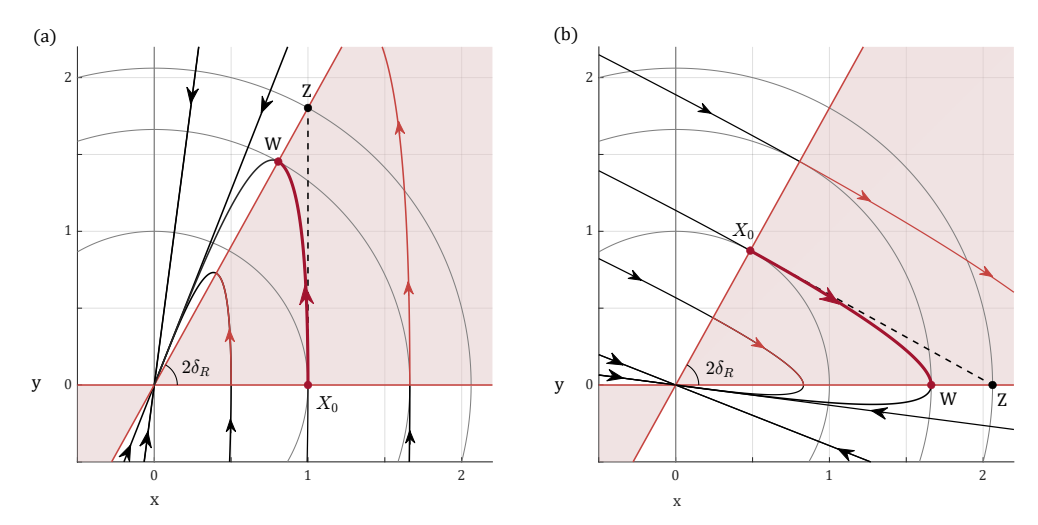


Fig. 11: Both (a) and (b) show the first quadrant phase portraits of a system in \mathcal{R} -zeroed form and illustrate the proof idea for bounding maximum amplification in Theorem 7.5. In (a), trajectories pass through the reactive region counter clockwise from $\phi_1 = 0$ to $\phi_2 = 2\delta_R$. The trajectory with initial condition $X_0 = (1,0)^T$ exits the reactive region at the point W which is closer to the origin than the point $Z = (1, \tan(2\delta_R))^T$. In (b), $\mathcal{T} < 0$ in the reactive region so trajectories pass through the reactive region clockwise from $\phi_2 = 2\delta_R$ to $\phi_1 = 0$. The trajectory with initial condition $X_0 = (\cos(2\delta_R), \sin(2\delta_R))^T$ exits the reactive region at the point W on the x-axis. The system in (a) corresponds to the original coefficient matrix $\begin{pmatrix} 0 & -8 \\ 0 & -3 \end{pmatrix}$ rotated into \mathbb{R} -zeroed form. The system in (b) corresponds to the original coefficient matrix $\begin{pmatrix} 0 & -8 \\ 0 & -3 \end{pmatrix}$; it has the same eigenvalues, reactive region, and relative eigenvector locations as the system in (a), but the midline m_T and orthovalues μ_1 and μ_2 are negative that of system (a).

Z where the line x=1 intersects $\theta=2\delta_R$. See Figure 11. Thus, by trigonometry and Corollary 6.6, the maximal amplification satisfies:

$$\rho_{max} = ||W|| < ||Z|| = \frac{1}{\cos(2\delta_R)} = -\frac{p}{m_R}.$$

The case when $\mathcal{T} < 0$ on the reactive region is proved similarly. In this case trajectories traverse the reactive region clockwise. One approach is to choose an initial condition on the line $\theta = 2\delta_R$. The calculations are slightly more delicate, but still straightforward. Another approach is to first conjugate with rotation to re-locate the reactive region to $\theta \in (-2\delta_R, 0) \cup (\pi - 2\delta_R, \pi)$, and then choose $X_0 = (1, 0)^T$ as before. See Figure 11(b).

REMARK. The estimate in Theorem 7.5 is sharp, in the sense that if $\lambda_1 \to 0$ and $m_T > 0$, the system approaches the degenerate case in which there is an attracting line of equilibria along $\theta = 2\delta_R$, and all other trajectories are parallel to the y-axis. If $m_T < 0$, the system has an attracting line of equilibria along $\theta = 0$ and all other trajectories approach $\theta = 0$ in paths perpendicular to the other orthovector at $\theta = 2\delta_R$. In both cases, W = Z and $\rho_{max} = -\frac{p}{m_R}$.

Theorem 7.5 gives an upper bound for ρ_{max} based on the reactivity radius, δ_R . In a reactive attractor with real eigenvalues, a bound on the reactivity radius can be determined, in turn, from the eigenvector separation radius, δ_T . In the following

corollary of Theorem 7.5, we use this fact to find an alternative (weaker) upper bound on ρ_{max} in terms of δ_T .

COROLLARY 7.6. If System 2.1 has a reactive attractor at the origin, with real eigenvalues, and eigenvector separation radius $\delta_T \in (0, \pi/2)$, then

$$\rho_{max} < \frac{1}{\sin(2\delta_T)} = \frac{p}{p_R}.$$

Proof. Since System 2.1 has real, negative eigenvalues, we know that $\mathcal{T}(\theta) \neq 0$ when $\mathcal{R}(\theta) > 0$, so $\mathcal{T}(\theta)$ is single signed on the reactive region. Thus, by splitting into the cases $0 < \delta_T < \pi/4$ and $\pi/4 < \delta_T < \pi/2$, it is straightforward to see that

$$2\delta_R \in (0, |\pi/2 - 2\delta_T|) \subset (0, \pi/2)$$

and hence, by trigonometry and Corollary 6.6,

$$\rho_{max} < \frac{1}{\cos(2\delta_R)} < \frac{1}{\cos(|\pi/2 - 2\delta_T|)} = \frac{1}{\sin(2\delta_T)} = \frac{p}{p_R}.$$

Remark. Corollary 7.6 supports our intuition that, as the eigenvectors in a reactive attractor converge to each other, the potential for reactivity driven amplification increases.

Theorem 7.5 and Corollary 7.6 are useful for providing a quick upper bound on the maximal amplification, ρ_{max} , admitted by System 2.1. In an upcoming paper, we show ρ_{max} can be calculated exactly by integrating $\mathcal{R}(\theta(t))$, with respect to time, as a trajectory traverses the reactive region. As stated in Theorem 7.7, the formula for ρ_{max} can be written in a variety of ways, each shedding a different light on what determines the maximal amplification.

Equation (7.1) shows how the balancing act between the transient and asymptotic dynamics of System (2.1) that yields the maximum amplification can be captured by an intertwining of the eigenvalues and orthovalues of A. By contrast, Equation (7.3) shows that, in the case of real eigenvalues, ρ_{max} that same balance is captured by the eigenvector and orthovector separations, δ_T and δ_R .

THEOREM 7.7. The maximal amplification, ρ_{max} , admitted by System 2.1 is determined by the eigenvalues and orthovalues of A as follows:

$$\rho_{max} = \left(\left(\frac{\lambda_1 \mu_2 + \lambda_2 \mu_1}{\lambda_1 \mu_1 + \lambda_2 \mu_2} \right)^{\left(\frac{\lambda_1 + \lambda_2}{\lambda_1 - \lambda_2} \right)} \left(\frac{\mu_1}{\mu_2} \right) \right)^{\frac{1}{2}}$$
 (7.1)

which can also be written:

$$\rho_{max} = \left(\left(\frac{m_R m_T - p_R p_T}{m_R m_T + p_R p_T} \right)^{\left(\frac{m_R}{p_R} \right)} \left(\frac{m_T + p_T}{m_T - p_T} \right) \right)^{\frac{1}{2}}$$
 (7.2)

In the case when A has real eigenvalues, ρ_{max} can also be determined from the eigenvector and orthovector separations:

$$\rho_{max} = \left(\left(\frac{\cos(2\delta_R + 2\delta_T)}{\cos(2\delta_R - 2\delta_T)} \right)^{-\left(\frac{\cos(2\delta_R)}{\sin(2\delta_T)}\right)} \left(\frac{\cos(2\delta_T) - \sin(2\delta_R)}{\cos(2\delta_T) + \sin(2\delta_R)} \right) \right)^{\frac{1}{2}}$$
(7.3)

8. Surfing the reactivity in nonautonomous systems. Theorem 7.5 showed that when System (2.1) has a reactive attractor, even though it can have arbitrarily large reactivity for almost any given set of eigenvectors or eigenvalues (Theorems 7.4 and 7.3), the maximum amplification, ρ_{max} , is bounded.

In this section we use the \mathcal{R} and \mathcal{T} framework to give new insight into the well-known but counter-intuitive fact that in a nonautonomous linear system, even if every 'frozen-time' system has a global attractor at the origin, the accumulation of radial growth can be unbounded.

To fix ideas, let A be a 2×2 matrix for which System (2.1) has a reactive attractor, and consider the nonautonomous linear system:

$$\frac{dX}{dt} = B_k(t)X = M_{kt}^{-1} A M_{kt} X. (8.1)$$

where M_{kt} is the rotation matrix defined in Equation (6.1). Note that the conjugation by M_{kt} has the effect of nonautonomously rotating the vector field generated by A clockwise with a fixed angular velocity, k.

Nonautonomous families of this form have been well studied. See, for example, the elegant survey by Josić and Rosenbaum [7], and the references therein. In Theorem 8.1, below, we recast Theorem 3.1 of [7] in the \mathcal{R} and \mathcal{T} framework.

Theorem 8.1. If the matrix A corresponds to a system with a reactive attractor, then System (8.1) is asymptotically repelling if and only if

$$-k \in (\mu_2, \mu_1) = (m_T - p_T, m_T + p_T)$$

where μ_2 and μ_1 are the orthovalues of A.

Before proving Theorem 8.1, let's build some intuition. For each fixed $s \in \mathbb{R}$, the frozen coefficient matrix $B_k(s)$ is a conjugation by rotation of A, and hence shares the same reactivity, ρ_1 , and reactive radius, δ_R , as A (Corollaries 6.5). Thus, at each frozen-time instant in the nonautonomous dynamics there is a region in which solutions are moving away from the origin, i.e. 'surfing' the reactivity. The intuition behind Theorem 8.1 is that if our nonautonomous rate of rotation, k, is compatible with the angular velocity in the reactive region, then the nonautonomous rotation and the underlying rotation of the vector field will trap solutions in the reactive region. These trapped solutions will then keep surfing the reactivity forever.

To cement this intuition, we first prove Lemma 8.2 showing that \mathcal{R} and \mathcal{T} respect matrix addition. We then prove Theorem 8.1 by moving from an inertial frame of reference to a co-rotating frame of reference, in which the the nonautonomous system can be represented by the sum of two *autonomous* linear systems: one representing the original matrix A, and the other representing the conjugation by rotation. We can then use the autonomous \mathcal{R} and \mathcal{T} approach to analyze the balance between the angular velocity, \mathcal{T}_A , within the reactive region of System (2.1), and the nonautonomous rotation rate, k, of System (8.1).

Lemma 8.2. Let A and B be two real 2×2 matrices. Then

$$\mathcal{R}_{A+B}(\theta) = \mathcal{R}_A(\theta) + \mathcal{R}_B(\theta)$$
$$\mathcal{T}_{A+B}(\theta) = \mathcal{T}_A(\theta) + \mathcal{T}_B(\theta).$$

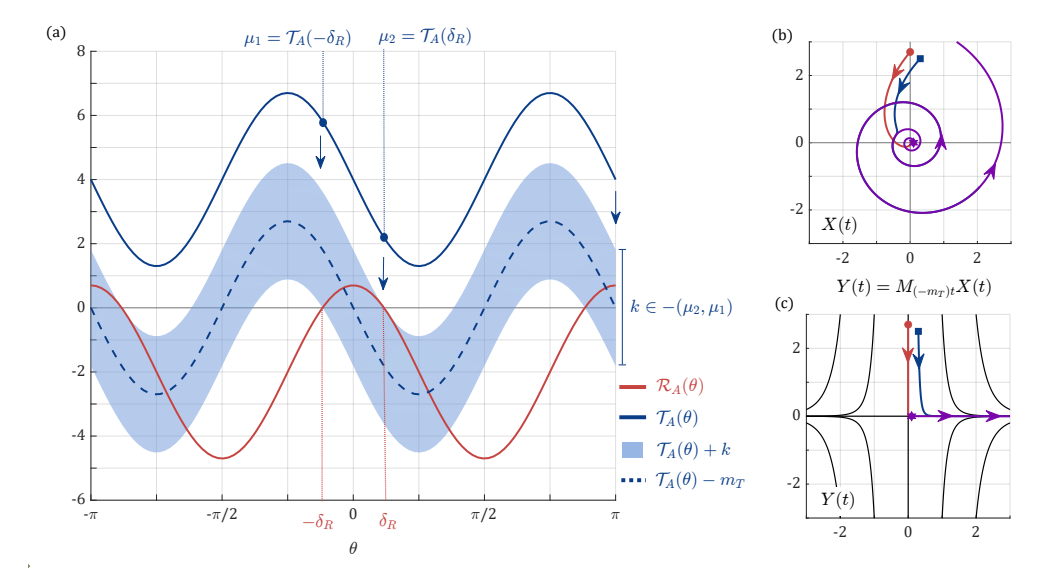


Fig. 12: To illustrate Theorem 8.1, we consider the nonautonomous rotation of the coefficient matrix $A = \begin{pmatrix} 0.7 & -4 \\ 4 & -4.7 \end{pmatrix}$. The radial and tangential components \mathcal{R}_A and \mathcal{T}_A of this constant coefficient system are plotted in solid lines in (a). Notice that $m_T = 4$, $m_R = -2$, and $\mu_{1,2} = \mathcal{T}_A(\mp \delta_R) \approx 4 \pm 1.8$. Part (a) also illustrates how shifting \mathcal{T}_A by $k \in -(\mu_2, \mu_1)$ pushes a root of the tangential curve into the reactive set $\mathcal{S}_R = (-\delta_R, \delta_R)$. If k is selected to be $-m_T = -4$ (the dashed dark blue curve), the resulting system, $\frac{dY}{dt} = (A - 4J)Y$, will have a symmetric saddle with eigenvectors at $\theta = 0$ and $\theta = \pi/2$ (corresponding to (b) and (c)). Part (b) shows three trajectory curves X(t) for System (8.1) with k = -4. The corresponding trajectories $Y(t) = M_{(-m_T)t}X(t)$ in the co-rotated autonomous system described by System (8.2) are depicted in (c). Note that the linear phase portrait has orthogonal eigenvectors on the axes and exhibits saddle behavior; the vector field has radial component given by $\mathcal{R}_A(\theta)$ and tangential component given by $\mathcal{T}_A(\theta) - m_T$ (dashed blue line in (a).

Proof. By Theorem 2.1,

$$\mathcal{R}_{A+B}(\theta)X + \mathcal{T}_{A+B}(\theta)X^{\perp} = (A+B)X$$

$$= AX + BX$$

$$= \mathcal{R}_{A}(\theta)X + \mathcal{T}_{A}(\theta)X^{\perp} + \mathcal{R}_{B}(\theta)X + \mathcal{T}_{B}(\theta)X^{\perp}$$

$$= (\mathcal{R}_{A}(\theta) + \mathcal{R}_{B}(\theta))X + (\mathcal{T}_{A}(\theta) + \mathcal{T}_{A}(\theta))X^{\perp}$$

and hence
$$\mathcal{R}_{A+B}(\theta) = \mathcal{R}_A(\theta) + \mathcal{R}_B(\theta)$$
 and $\mathcal{T}_{A+B}(\theta) = \mathcal{T}_A(\theta) + \mathcal{T}_A(\theta)$.

Proof of Theorem 8.1. Since the nonautonomous conjugation rotates at rate k, we move into a co-rotating frame of reference by choosing new coordinates that rotate at the same rate, $Y = M_{kt}X$. Then:

$$\frac{dY}{dt} = \frac{d}{dt} [M_{kt}X] = \frac{d}{dt} [M_{kt}]X + M_{kt} \frac{dX}{dt}$$

$$= \begin{pmatrix} 0 & -k \\ k & 0 \end{pmatrix} M_{kt}X + AM_{kt}X$$

$$= (A+kJ)Y = CY. \tag{8.2}$$

Equation 8.2 means that in the co-rotating coordinate frame, the nonautonomous system is represented by an *autonomous* linear system, and, by Lemma 8.2, the radial and tangential components of the dynamics are given by

$$\mathcal{R}_C(\theta) = \mathcal{R}_A(\theta)$$
 and $\mathcal{T}_C(\theta) = \mathcal{T}_A(\theta) + k$.

So, in the new co-rotating coordinates, the nonautonomous rotation imposed by conjugation by M_{kt} in System (8.1) manifests as a vertical translation of \mathcal{T}_A . See Figure 12

The asymptotic radial dynamics of (8.1) are equivalent to that of (8.2) via the change of coordinates $X(t) = M_{kt}^{-1}Y(t)$ since ||X(t)|| = ||Y(t)||. To complete the proof, we must simply consider when the autonomous dynamics of System (8.2) are asymptotically repelling.

Since $m_R < 0$, System (8.2) must generically be either an attractor or a saddle. It is a saddle if and only if there exists a positive real eigenvalue $\lambda_1 > 0$. By Corollary 4.1 and Definitions 3.5 and 3.6, $\lambda_1 > 0$ if and only if the corresponding eigenvector angle is located in the reactive set, S_R . It follows that System (8.2) has a saddle if and only if $-k \in T_A(S_R) = (\mu_2, \mu_1)$, since that $\mathcal{T}_C(\theta) = 0$ if and only if $\mathcal{T}_A(\theta) = -k$ for some $\theta \in S_R$.

Theorem 8.1 gives us a starting point for understanding how reactivity can accumulate in nonautonomous systems to produce asymptotic behavior that differs from the asymptotic behavior of the corresponding frozen-time systems. The proof of Theorem 8.1 is just one example of how our radial and tangential framework helps to fix a clear perspective from which to analyze transient effects.

Figure 12 gives an example of how this is applied for a system in \mathcal{R} -centered form.

REFERENCES

- M. G. Neubert and H. Caswell, "Alternatives to resilience for measuring the responses of ecological systems to perturbations," Ecology, vol. 78, no. 3, pp. 653–665, 1997.
- [2] S. Townley and D. J. Hodgson, "Erratum et addendum: transient amplification and attenuation in stage-structured population dynamics," <u>Journal of Applied Ecology</u>, vol. 45, no. 6, pp. 1836–1839, 2008.
- [3] A. Hastings, K. C. Abbott, K. Cuddington, T. Francis, G. Gellner, Y.-C. Lai, A. Morozov, S. Petrovskii, K. Scranton, and M. L. Zeeman, "Transient phenomena in ecology," <u>Science</u>, vol. 361, no. 6406, p. eaat6412, 2018.
- [4] T. B. Francis, K. C. Abbott, K. Cuddington, G. Gellner, A. Hastings, Y.-C. Lai, A. Morozov, S. Petrovskii, and M. L. Zeeman, "Management implications of long transients in ecological systems," Nature Ecology & Evolution, vol. 5, no. 3, pp. 285–294, 2021.
- [5] K. Meyer, A. Hoyer-Leitzel, S. Iams, I. Klasky, V. Lee, S. Ligtenberg, E. Bussmann, and M. L. Zeeman, "Quantifying resilience to recurrent ecosystem disturbances using flow-kick dynamics," Nature Sustainability, vol. 1, no. 11, pp. 671–678, 2018.
- [6] A. Haslam, "Classifying flow-kick equilibria: Reactivity and transient behavior in the variational equation," Bachelor's Thesis, Bowdoin College, https://digitalcommons.bowdoin.edu/honorsprojects/191, 2020.
- [7] K. Josić and R. Rosenbaum, "Unstable solutions of nonautonomous linear differential equations," SIAM review, vol. 50, no. 3, pp. 570-584, 2008.
- [8] J. Mierczynski, "Instability in linear cooperative systems of ordinary differential equations," SIAM Review, vol. 59, no. 3, pp. 649–670, 2017.
- [9] S. D. Lawley, J. C. Mattingly, and M. C. Reed, "Sensitivity to switching rates in stochastically switched odes," Communications in Mathematical Sciences, 2013.
- [10] N. S. Nise, Control systems engineering. John Wiley & Sons, 2019.
- [11] K. Ogata, Modern control engineering. Prentice hall, 2010.
- [12] D. J. Higham and L. N. Trefethen, "Stiffness of odes," <u>BIT Numerical Mathematics</u>, vol. 33, pp. 285–303, 1993.

- [13] P. D. Harrington, M. A. Lewis, and P. van den Driessche, "Reactivity, attenuation, and transients in metapopulations," SIAM Journal on Applied Dynamical Systems, vol. 21, no. 2, pp. 1287–1321, 2022.

 [14] M. W. Hirsch, S. Smale, and R. L. Devaney, Differential equations, dynamical systems, and an introduction to chaos. Academic press, 2012.